ADVANCES IN ATOMIC AND MOLECULAR PHYSICS, VOL. 19

HIGH-RESOLUTION SPECTROSCOPY OF STORED IONS

D. J. WINELAND and WAYNE M. ITANO

Time and Frequency Division
National Bureau of Standards
Boulder, Colorado

R. S. VAN DYCK, JR.

Department of Physics
University of Washington
Seattle, Washington

I. Introduction 136
A. Scope of the Present Article 136
B. The Method 136
II. Ion Storage Techniques 137
A. The Paul (rf) Trap 138
B. The Penning Trap 143
C. The Kingdon Trap 145
D. Ion Creation 147
E. Ion Detection 148
F. Polarization Production/Monitoring 148
G. Other Types of Traps 149
III. Lepton Spectroscopy 149
A. Historical Perspective 149
B. Electron Geonium Experiment 151
C. Positron Geonium Experiment 156
IV. Mass Spectroscopy 159
A. Introduction 159
B. First Mainz Experiment 160
C. Second Mainz Experiment 162
D. University of Washington Experiment 164
V. Atomic and Molecular Ion Spectroscopy 166
A. Optical Atomic Ion Spectroscopy 166
B. Laser Cooling 167
C. Microwave and rf Atomic Ion Spectroscopy 171
D. Application to Frequency Standards 175
E. Molecular Ion Spectroscopy 176
VI. Negative Ion Spectroscopy 176
A. Atoms 177

ISBN 0-12-003819-6

B. Molecules 179
VII. Radiative Lifetime Measurements 180
References 181

I. Introduction

A. Scope of the Present Article

In this article we attempt to give a review of spectroscopic experiments that have employed the stored ion technique. This review will be biased toward very high-resolution experiments since this is the authors' area of interest. We hope that a description of these high-resolution experiments will illustrate the current state of the art and indicate possible achievements in the future. In this article collision experiments in the usual sense (charge exchange, ion–molecule reactions, etc.) will specifically be excluded—we are primarily interested in photon–ion interactions and will include such topics as spectroscopy of atomic ions, mass spectroscopy using resonant excitation, and measurement of radiative decay times. To make this article more tractable, we do not discuss the interesting spectroscopy that has been done in conjunction with fusion plasma studies or high-energy storage rings. We also omit discussion of the interesting studies of the dynamics of water droplets (Owe Berg and Gaukler, 1969) and of aerosols initiated by C. B. Richardson (private communication, 1982).

The most complete previous review has been given by Dehmelt (1967, 1969) and is still "the" reference for someone starting in this field. Schuessler (1979) has given a review which concentrated on the ion storage exchange collision (ISEC) method in an rf quadruple trap. More recently, Dehmelt (1983) has given a review/introduction as part of a NATO Advanced Study Institute. Todd *et al.* (1976) have given a review of rf traps. In addition, various other partial reviews have also been given (Dehmelt, 1975, 1976, 1981a,b; Minogin, 1982; Neuhauser *et al.* 1981; Toschek and Neuhauser, 1981; Werth, 1982; Wineland *et al.*, 1981b; Wineland, 1983).

Necessarily, there will be some overlap of this review with previous ones; we will tend to rely on these other reviews which have extensively covered some of the techniques such as the ISEC method (Dehmelt, 1969; Schuessler, 1979).

B. The Method

Probably the main advantage of the stored ion techniques is that the ideal of an unperturbed species at rest in space is approached to a high degree.

Specifically, charged particles such as electrons and atomic ions can be stored for long periods of time (essentially indefinitely) without the usual perturbations associated with confinement (for example, the perturbations due to collisions with walls or buffer gases in a traditional optical pumping experiment).

Unfortunately (and necessarily), there is a price to be paid for this property of long storage times with small perturbations—the number of particles that can be stored is typically small (approximately 10^6 or less for a "trap" with centimeter dimensions); the resulting low densities are ultimately governed by the competition between space-charge repulsion and the confining electromagnetic forces obtained under normal laboratory conditions. It should be noted that if we could obtain the high trapping fields necessary to obtain high densities, then we would lose one of the advantages of the technique because, for example, Stark shifts due to confinement would cause problems in very high-resolution work.

As a consequence of the low numbers obtained, many types of experiments may be precluded—for example, spectroscopic experiments on complex molecular ions where only a small fraction of the ions are in a given state. However, in spite of the low numbers obtained, sensitive techniques have been developed to detect simple species such as electrons and atomic ions, so that *single* electrons (Wineland *et al.*, 1973; Van Dyck *et al.*, 1978) and atomic ions (Neuhauser *et al.*, 1980; Wineland and Itano, 1981; Nagourney *et al.*, 1982, 1983; Ruster *et al.*, 1983) can be observed.

In Section II, trapping methods are discussed. In Section III, the electron–positron (g-2) experiments are discussed. These experiments may be the least general of those covered, but a large part of the new developments in the stored ion technique have occurred here. In Section IV applications to mass spectroscopy are discussed. Section V discusses experiments on atomic and molecular ion spectroscopy. Sections VI and VII discuss negative ion experiments and lifetime studies.

II. Ion Storage Techniques

Four types of "traps" have been most commonly used for high-resolution work: the Paul (or rf) trap, the Penning trap, the Kingdon (or electrostatic trap), and the magnetostatic trap (magnetic bottle). Magnetic bottles have not been used extensively for high-resolution work because the trapping relies on the use of inhomogeneous magnetic fields, thus causing inhomogeneities and broadening in field-dependent transitions. An exception to

this is the high-resolution electron–positron magnetic moment measurements done by Crane, Rich, and their colleagues (Rich and Wesley, 1972). For the sake of brevity however, magnetic confinement devices will not be discussed further.

A. The Paul (rf) Trap

The Paul or rf trap has the advantage that the trapped ions are bound in a (pseudo) potential well in all directions and no magnetic fields are required for confinement. It has the capability in practice to provide tighter confinement than the Penning trap, but the phenomenon of "rf heating" has been a limitation in some experiments.

1. Theory

The "ideal" Paul trap (Fisher, 1959; Wuerker *et al.*, 1959a) uses three electrodes in a vacuum apparatus as shown in Fig. 1. These electrodes are conjugate hyperboloids of revolution about the z axis, thus allowing a description of the potential in cylindrical coordinates. In general, both a static potential and an alternating potential of frequency Ω are applied between the ring and endcaps, so that

$$\phi(r, z) = \frac{U_0 + V_0 \cos \Omega t}{r_0^2 + 2z_0^2}(r^2 - 2z^2) \tag{1}$$

where r_0 and z_0 are defined in Fig. 1. The electrode surfaces are assumed to be equipotentials of Eq. (1), and we assume $\phi = 0$ at the center of the trap.

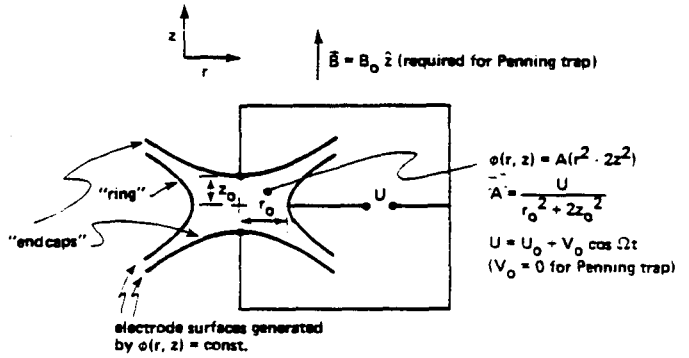

FIG. 1. Schematic representation of the electrode configuration for the "ideal" Paul or Penning trap. Electrode surfaces are figures of revolution about the z axis and are equipotentials of $\phi(r, z) = A(r^2 - 2z^2)$.

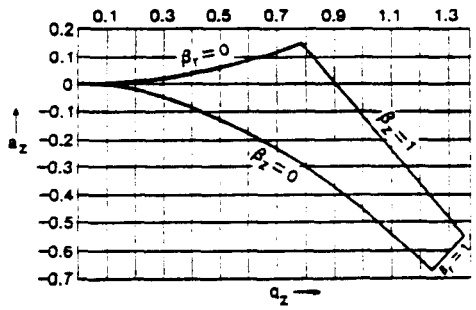

FIG. 2. Theoretical stability diagram for the Paul trap. The region bounded by the solid line represents the values of a_z and q_z giving stable confinement. The validity of this stability diagram has been confirmed in various experiments (see text).

The equations of motion for a positive ion take the form of a Mathieu equation (McLachlan, 1947):

$$\frac{d^2x_i}{d\tau^2} + (a_i - 2q_i \cos 2\tau)x_i = 0$$

where

$$-a_z = +2a_r = 16qU_0/m\Omega^2(r_0^2 + 2z_0^2)$$
$$+q_z = -2q_r = 8qV_0/m\Omega^2(r_0^2 + 2z_0^2)$$

m is the ion mass, $\tau = \Omega t/2$, and q is the ion charge.

Certain values of a_i and q_i lead to stable bounded motion; these values are bounded by the curve on the stability diagram shown in Fig. 2. Other regions of stability exist (Fisher, 1959; Wuerker *et al.*, 1959a; Dawson, 1980); only the first region of stability, which is shown, is usually used. The perimeter of this curve is determined by the values $\beta_i = 1$ and 0, where $\beta_i^2 = a_i + q_i^2/2$.

A qualitative explanation for the binding due to the rf field in the traps is as follows (Wuerker *et al.*, 1959a; Dehmelt, 1967): For Ω sufficiently large (i.e., $\beta \ll 1$) an ion experiences an rf electric field such that its motion (the "micromotion") is 180° out of phase with respect to the electric force. Because the electric field is inhomogeneous, the force averaged over one period ($T = 2\pi/\Omega$) of the micromotion is in a direction of weaker field amplitude (independent of the sign of the charge), i.e., toward the center of the trap. For Ω sufficiently high, this restoring force gives rise to a pseudopotential (Dehmelt, 1967):

$$\psi(r, z) = \frac{qV_0^2}{m\Omega^2(r_0^2 + 2z_0^2)^2}[(\bar{r})^2 + 4(\bar{z})^2] \qquad (U_0 = 0) \qquad (2)$$

where $\bar{r}$ and $\bar{z}$ are the positions of the ion averaged over T, and q is the ion charge. The resulting "secular" motion (for $\bar{r}$ and $\bar{z}$) is harmonic with frequencies $\bar{\omega}_z = 2\bar{\omega}_r = 2\sqrt{2}qV_0/[\Omega m(r_0^2 + 2z_0^2)]$.

The addition of the static potential U_0 alters the well depth directly so that we must add the potential

$$\phi_{DC} = \frac{U_0}{r_0^2 + 2z_0^2}(r^2 - 2z^2) \tag{3a}$$

to the expression for the pseudopotential. This yields an overall effective (harmonic) potential:

$$\begin{aligned}\phi(r, z) = \psi + \phi_{DC} &= \frac{k_r}{2q}(\bar{r})^2 + \frac{k_z}{2q}(\bar{z})^2 \\ &= \left[\frac{qV_0^2}{m\Omega^2(r_0^2 + 2z_0^2)^2} + \frac{U_0}{r_0^2 + 2z_0^2}\right](\bar{r})^2 \\ &\quad + \left[\frac{4qV_0^2}{m\Omega^2(r_0^2 + 2z_0^2)^2} - \frac{2U_0}{r_0^2 + 2z_0^2}\right](\bar{z})^2 \end{aligned} \tag{3b}$$

A special case is when $U_0 = qV_0^2/m\Omega^2(r_0^2 + 2z_0^2)$, which gives rise to a "spherical" potential where $\phi(r, z) \propto (\bar{r})^2 + (\bar{z})^2$. It is sometimes useful to describe the traps in terms of well depths in the r and z directions; for example, we can define

$$D_r = \phi(r = r_0, 0) - \phi(0, 0)$$

$$D_z = \phi(0, z = z_0) - \phi(0, 0)$$

For the more general potential of Eq. (3b), the secular oscillation frequencies are $\bar{\omega}_r = (k_r/m)^{1/2}$ and $\bar{\omega}_z = (k_z/m)^{1/2}$.

As an example of operating conditions, we take the data from Major and Werth (1978) for $^{199}Hg^+$ ions. Here $r_0 = \sqrt{2}z_0 = 1.129$ cm, $\Omega/2\pi = 524$ kHz, $U_0 = +8$ V (ring electrode biased positively with respect to the end-caps), and $V_0 = 297$ V. This gives $a_z = -0.024$, $q_z = 0.432$, $\bar{\omega}_r/2\pi = 49$ kHz, $\bar{\omega}_z/2\pi = 69$ kHz. This particular choice of parameters also gives $D_r = D_z = 12$ eV. Very small traps have been used to provide tight confinement for single ion detection. From Neuhauser *et al.* (1978b), $V_0 \cong 200$ V and $r_0 = \sqrt{2}z_0 = 354\ \mu$m.

The potential of Eq. (1) is said to be ideal because it has the simplest form which satisfies Laplace's equation and has the desired symmetry (independent of azimuthal angle and reflection symmetry about $z = 0$). For the same symmetry, deviations from the ideal potential introduce higher-order terms; the first of these has spatial dependence $(3r^4 - 24r^2z^2 + 8z^4)$ and introduces anharmonicities in the secular frequencies $\bar{\omega}_z$ and $\bar{\omega}_r$. These deviations can

come about due to imperfections in the electrodes such as holes for observation and the fact that the surfaces must be truncated. They are obviously introduced for a trap with simple cylindrical geometry (Benilan and Audoin, 1973; Bonner *et al.*, 1977) or spherical electrodes (O and Schuessler, 1980a), but the region of stability is not substantially altered (Benilan and Audoin, 1973; Mather *et al.*, 1980).

We note that the choice of r_0/z_0 is in principle arbitrary and not inferred from Laplace's equation as has been implied (Dawson and Whetten, 1968; Todd *et al.*, 1976; Bonner *et al.*, 1977). Of course, to yield the ideal potential of Eq. (1), the electrode surfaces must be equipotentials of Eq. (1) and therefore both the ring and endcaps must asymptotically approach the surfaces generated by $z = \pm r/\sqrt{2}$. The choice $r_0^2 = 2z_0^2$ can be made so that the ring and endcap surfaces are equidistant from these asymptotes for large r and z. Knight (1983, also private communication) has also pointed out that the stability diagram is independent of the choice of r_0/z_0 as long as a_i and q_i are determined from the formulas given previously.

The motion of a single ion in the trap is described by the solution of the Mathieu equation. For many ions in the trap, distribution functions can be obtained under various assumptions. Assuming no collisions or space charge, phase space dynamical techniques have been used to calculate distribution functions and give fairly good agreement with observed data (Todd *et al.*, 1980b). For the long-term storage desired in spectroscopic experiments, ion–ion and ion–neutral collisions play an important role. In general, this gives rise to what is called "rf heating"—a process which couples kinetic energy from the micromotion into the secular motion (Church and Demelt, 1969). Elastic collisions with background neutrals will either produce heating if the neutrals are heavy with respect to the ions or an effective cooling (viscous drag) if the neutrals are light (Dehmelt, 1967). This has been examined in detail theoretically (André and Vedel, 1977; Dawson and Lambert, 1975; André *et al.*, 1979; F. Vedel *et al.*, 1981, 1983; M. Vedel *et al.*, 1981), predicting Gaussian density distributions. In addition, resonant charge exchange with the parent neutral may provide a stabilizing influence (Bonner *et al.*, 1976; Dawson, 1980). In many experiments done at high vacuum, it appears that the dominant heating mechanism is due to ion–ion collisions (Dehmelt, 1967). Such heating is not well understood but may arise from the presence of impurity ions or from imperfections in the trap electrodes.

Space charge will have a destabilizing effect on an ion cloud, that is, the wells become more shallow due to the presence of other ions. If the secular motion is "frozen," then the ions form around the center of the trap so that the net electric field an ion experiences inside the cloud is zero. Therefore, following Dehmelt (1967), $\phi + \phi_i = \text{constant}$, where ϕ_i is the potential from

the ion cloud. Applying the Laplacian to this equation, we find that the ion cloud has uniform (maximum) density ρ given by

$$\rho_{max} = \frac{1}{4\pi}\nabla^2\phi = \frac{3qV_0^2}{\pi m\Omega^2(r_0^2 + 2z_0^2)^2} \tag{4}$$

For the conditions of Major and Werth (1978), this leads to a maximum density of $n_{max} = \rho_{max}/q = 4 \times 10^7$ cm^{-3}.

2. Experiments

The kinematics of ion motion have been verified in the original experiments of Wuerker *et al.* (1959a), where charged aluminum dust particles (ca. 20 μm diameter) were suspended in an rf trap and illuminated so that the paths could be observed. In these beautiful experiments the particles could also be observed to crystallize into lattices when the background gas pressure was increased to cause cooling.

For atomic ions, the validity of the stability diagram has been verified in experiments. Trapping efficiencies have been measured by monitoring the relative intensity of laser-induced fluorescence light from Ba^+ ions (Iffländer and Werth, 1977a; Plumelle *et al.*, 1980). Temperature was monitored via the Doppler broadening of the resonance light. Trapping efficiencies have also been measured by observing storage times as a function of trapping conditions (M. Vedel *et al.*, 1981). Temperature also has been measured by the bolometric method (Church and Dehmelt, 1969) discussed below. In addition, the cooling efficiency of buffer gases has also been observed (Vedel, 1976; Dawson, 1980; Plumelle *et al.*, 1980; Schaaf *et al.*, 1981; Ruster *et al.*, 1983). In the experiments of Plumelle *et al.* (1980) using helium buffer gas, trapping times of several days have been observed (Plumelle, 1979; see also Blatt and Werth, 1983). Density measurements have also been made optically (Knight and Prior, 1979; Schaaf *et al.*, 1981), indicating a Gaussian density distribution. The results of these experiments and those of Iffländer and Werth (1977a) and of Church and Dehmelt (1969) showed that the ion temperature was approximately equal to a constant fraction (ca. 0.1) of the well depth. These measurements are also in agreement with the measurement of ion loss based on evaporation (Dehmelt, 1983). Ion–neutral collision studies based on ion creation and loss are given by Todd *et al.* (1976) and can be used to infer ion energies. In the experiments of Knight and Prior (1979) the cloud radius (and therefore the ion energy) was shown to be fairly independent of ion number, indicating that ion–ion rf heating was not important. This was not the case for the very small clouds observed by Neuhauser *et al.* (1980), where a large increase in cloud radius was

observed as the ion number increased. In these experiments, however, ion densities were as high as 10^9 cm^{-3}, increasing the importance of ion–ion collisions.

The destabilizing effect of space charge has been observed by Todd *et al.* (1980a) and Neuhauser *et al.* (1978b). However, the densities predicted from the model where the secular motion is cold have not been observed. Usually the densities are one to two orders of magnitude less than this prediction, presumably due to rf heating. Increased densities have been observed by simultaneously storing positive and negative ions (Major and Schermann, 1971), but ion–ion heating would be expected to be important for high densities.

B. The Penning Trap

The Penning trap has the disadvantages of the typically large magnetic fields (larger than about 0.1 T) required and the fact that the motion (magnetron motion) is in an unstable equilibrium in the trap. An important practical advantage is that parasitic heating mechanisms (like rf heating in the Paul trap) are nearly absent. It may also be the clear choice for studies of magnetic field-dependent structure.

1. Theory

The Penning trap (Penning, 1936) uses the same electrode configuration as the rf trap (Fig. 1), but we set V_0 equal to zero in Eq. (3b) such that the charged species see only a static potential well along the z axis given by Eq. (3a). This causes a repulsive potential in the x–y plane which can be overcome by superimposing a static magnetic field along z ($\mathbf{B} = B_0\hat{z}$). For a single ion in the trap (or neglecting space charge) the equations of motion are (Harrison, 1959; Byrne and Farago, 1965) as follows:

$$\ddot{z} + \omega_z^2 z = 0, \qquad \dot{\mathbf{r}} = \tfrac{1}{2}\omega_z^2 \mathbf{r} - i\omega_c \dot{\mathbf{r}}$$

where $\mathbf{r} = x + iy$, $\omega_z^2 = 4qU_0/m(r_0^2 + 2z_0^2)$, and $\omega_c = qB/mc$. Therefore

$$z = z_0 \cos \omega_z t \text{ and } \mathbf{r} = \mathbf{r}_c e^{-i\omega_c' t} + \mathbf{r}_m e^{-i\omega_m t} \tag{5a}$$

where

$$\begin{Bmatrix} \omega_c' \\ \omega_m \end{Bmatrix} = \tfrac{1}{2}\omega_c \begin{Bmatrix} + \\ - \end{Bmatrix} \left[\left(\frac{\omega_c}{2}\right)^2 - \frac{\omega_z^2}{2} \right]^{1/2} \tag{5b}$$

Some useful expressions are $\omega^2 + \omega_z^2/2 = \omega_c\omega$ ($\omega = \omega_m$ or ω_c'), $\omega_c' + \omega_m = \omega_c$, and $\omega_c' \omega_m = \omega_z^2/2$. Quantum mechanical solutions have also been

given (Sokolov and Pavlenko, 1967; Gräff *et al.*, 1968; Van Dyck *et al.*, 1978; Itano and Wineland, 1982); this description is important for the single-electron experiments. Representative values of parameters might be $r_0 = \sqrt{2}z_0 = 0.5$ cm, $B = 2.0$ T, $U_0 = 2$ V. For electrons, $\omega_c/2\pi = \nu_c \cong 55.9$ GHz, $\nu_z = 26.7$ MHz, and $\nu_m = 6.36$ kHz. For $m = 100$ u (atomic mass units) ions, $\nu_c = 305$ kHz, $\nu_z = 62.3$ kHz, and $\nu_m = 6.50$ kHz. It should be noted that the magnetron motion [the $\mathbf{r}_m \exp(-i\omega_m t)$ term in Eq. (5a)] is in unstable equilibrium in the trap. Therefore, if collisions with background neutrals occur, the ions will diffuse out of the trap. For example, when the magnetron velocity is much less than the cyclotron velocity, elastic collisions with heavy neutrals cause r_m to random walk in the $x-y$ plane with step size approximately equal to r_c. In practice however, this is not a limitation because ions can be stored for days in an apparatus at room temperature (Wineland *et al.*, 1978; Drullinger *et al.*, 1980) and electrons for weeks (Dehmelt and Walls, 1968; Ekstrom and Wineland, 1980) in an apparatus at 80 K. Moreover the technique of sideband or radiation pressure cooling (Van Dyck *et al.*, 1978; Itano and Wineland, 1982) can reverse this diffusion process.

Ion–ion collisions can also cause the cloud to spread; however, this spreading is limited because the total canonical angular momentum of the system must be conserved (Wineland and Dehmelt, 1975c; O'Neil and Driscoll, 1979). For very cold clouds (i.e., axial and cyclotron modes at low temperature) this leads to clouds of nearly uniform density (O'Neil and Driscoll, 1979; Prasad and O'Neil, 1979), which for the Penning trap geometry implies that the cloud is a uniformly charged ellipsoid having the potential

$$\phi_i(r, z) = -\tfrac{2}{3}\pi\rho(ar^2 + bz^2) \tag{6}$$

where from Poisson's equation, $2a + b = 3$.

If the voltage U_0 applied to the electrodes becomes too high, then the radial electric field is high enough to overcome the $qv \times B/c$ magnetic force and the ions strike the ring electrode in exponentially increasing orbits [the argument of the square root in Eq. (5b) becomes negative.] For singly ionized atoms (or electrons) the voltage where this occurs is given by $V_c \cong 1200B^2(r_0^2 + 2z_0^2)/M$, where V_c is in volts, B is in tesla, M is the mass in u, and dimensions are in centimeters. This same mechanism limits the densities achievable in the Penning trap since space charge also gives radial electric fields. Assuming the ion cloud is a uniformly charged ellipsoid as discussed above, the r motion of an individual ion is now given by Eq. (5a) with

$$\begin{Bmatrix} \omega_c' \\ \omega_m \end{Bmatrix} = \frac{\omega_c}{2} \begin{Bmatrix} + \\ - \end{Bmatrix} \left[\left(\frac{\omega_c}{2}\right)^2 - \frac{\omega_z^2}{2} - \frac{4\pi q\rho a}{3m} \right]^{1/2} \tag{7}$$

where ω_z is the axial frequency for a single ion in the trap. The maximum density allowable (argument of the square root term kept positive) is given by [using $\phi_i(z) = -\phi_T(z)$] $n = p/q < B^2/8\pi c^2 m$ or $n < 2.7 \times 10^9 B^2/M$, where B is in tesla and M is the mass in u. For $B = 1$ T, $M = 100$ u, $n < 2.7 \times 10^7$ cm^{-3}.

In the refined work of electron–positron and mass spectroscopy, it is desirable to make the trap as nearly quadratic as possible. Assuming the trap has the desired symmetry, the fourth-order term (proportional to $3r^4 - 24r^2z^2 + 8z^4$) in the potential can be canceled out with correction electrodes (Van Dyck *et al.*, 1976). If the magnetic field is tilted with respect to the trap axis and the potential is imperfect but has the form $[r^2 - \epsilon(x^2 - y^2) - 2z^2]$, then the relation $(\omega_c')^2 + \omega_z^2 + \omega_m^2 = \omega_c^2$ will still hold (Brown and Gabrielse, 1982; see also Borodkin, 1978; O *et al.*, 1982).

2. *Experiments*

The main aspects of the theory have been confirmed. This has been done to a very high level in the electron–positron experiments discussed below. For clouds of ions the coupling between modes can be strong (energy transfer times of milliseconds), but the observed frequencies of motion for small clouds are essentially the free space values since only the center-of-mass motion is usually excited (Wineland and Dehmelt, 1975a,c).

Radial transport due to collisions with background neutrals seems to be reasonably well understood (Walls, 1970; McGuire and Fortson, 1974; Jeffries, 1980; deGrassie and Malmberg, 1980; Malmberg and Driscoll, 1980), but transport from ion–ion collisions is not so well understood. This may be caused by plasma oscillation-induced transport. Recent measurements on laser-cooled ion clouds (Bollinger and Wineland, 1983) indicate that they are approximately ellipsoidal in shape and of constant density, in agreement with prediction (Prasad and O'Neil, 1979).

C. The Kingdon Trap

The Kingdon trap (Kingdon, 1923) has the advantage of being simpler than the Paul or Penning trap, requiring only a dc voltage for trapping. Since a potential minimum in free space cannot exist for purely electrostatic fields, the Kingdon trap relies on angular momentum of the ions about a central axis to provide dynamical stability.

Usually, the Kingdon trap has the same symmetry of the Paul and Penning traps: A central wire is surrounded by an outer cylinder as shown in Fig. 3. Perhaps the most desirable potenial takes the form suggested by Prior

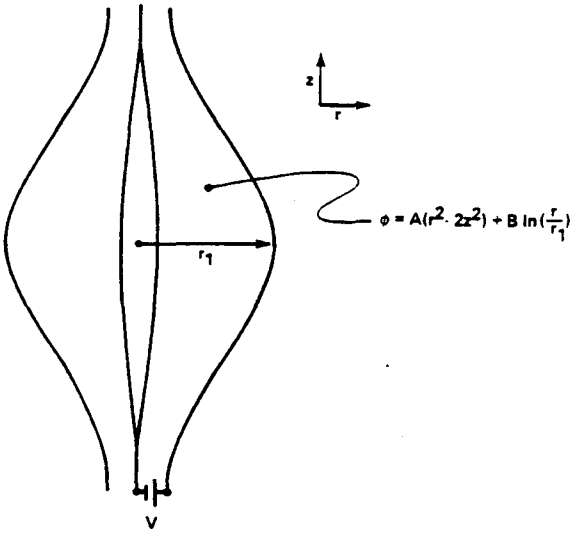

FIG. 3. Schematic representation of the electrode configuration for the "ideal" Kingdon trap. Electrode surfaces are figures of revolution about the z axis and are equipotentials of ϕ. In practice, the central electrode is made as thin as possible to reduce the chance of ions colliding with it.

(Knight, 1981), where

$$\phi = A(r^2 - 2z^2) + B \ln(r/r_1) \tag{8}$$

In this case, the motion is harmonic along z; therefore, detection of ω_z can provide mass analysis. Figure 3 shows a trap which is formed from equipotentials of Eq. (8); in practice, the central electrode would be much thinner but must still conform to an equipotential of Eq. (8) in order to preserve the harmonic well along z. The equations of motion for the $x-y$ plane are not solvable analytically, but the motion is basically composed of precessing orbits about the z axis (Hooverman, 1963). Lewis (1982) has analyzed the case of nearly circular orbits in a cylindrical trap. Storage times in such a trap should be shorter because a single collision with a background neutral is sufficient to cause an ion to collide with the center electrode and be lost. Nevertheless, with a trap whose electrodes approximate equipotentials of Eq. (8), trapping times of about 1 sec were achieved by Knight (1981) at a pressure of 10^{-6} Pa ($\cong 10^{-8}$ Torr). (The center electrode was 100-μm-diameter wire.)

The case of an axial magnetic field superimposed along the z axis has been investigated theoretically and experimentally (on He^+)(Johnson, 1983; Lewis, 1983); in this case storage times should increase dramatically. Ions

will eventually be lost by diffusing in toward the center electrode: therefore, storage times should be comparable to those of the Penning trap. However, the frequency of the drift motion about the center of the trap will depend on the distance from the z axis; for the Penning trap this drift (magnetron) frequency is independent of radial position (neglecting nonuniform space charge) and may be part of the reason for the slow evolution of the ion cloud under the influence of ion–ion collisions.

Prior and his colleagues have used the Kingdon traps extensively for spectroscopic studies (Prior, 1972; Prior and Wang, 1977; see also Vane *et al.*, 1981). Lewis (1983) has proposed to study the Aharonov–Bohm effect in a Kingdon trap.

D. Ion Creation

Certainly, the prevalent method for creating ions is from direct ionization of neutrals inside the trap by an externally injected electron beam. However, many times it is desirable to rid the trap of extraneous ions. In the rf trap this can be accomplished by operating the trap in the "mass-selective" mode (i.e., near the bottom of the stability diagram shown in Fig. 2). For the Penning trap, high-mass ions may be excluded by exceeding the "critical" voltage (Section II,B.1). For both traps, strong resonant excitation at the various motional frequencies can be used to drive unwanted ions from the trap.

If an ion is injected into the trap from the outside, it must lose energy inside the trap or it will eventually be lost. Such a scheme utilizing radiative energy loss has been successfully realized for positrons (Dehmelt *et al.*, 1978; Schwinberg *et al.*, 1981c) and various "catching" schemes have been proposed (see, for example, Todd *et al.*, 1976; O and Schuessler, 1981, 1982; Schuessler and O, 1981, and references therein).

Other possibilities for ion creation include photoinduced ion pair formation (Major and Schermann, 1971) and dissociative attachment for negative ion production (Blumberg *et al.*, 1978). Blatt *et al.* (1979) have demonstrated capture of Ba^+ ions from surface ionization followed by slowing down with a high-pressure helium buffer gas. Coutandin and Werth (1982; see also Blatt *et al.*, 1982) have demonstrated a technique whereby ions from an external source are first caught on a Pt ribbon. The neutrals are then evaporated from the ribbon and reionized inside the trap. They report overall efficiency of 10^{-5} and indicate that a significant increase in this number is possible. Knight (1981) reports capture of large numbers of ions from laser-produced plasmas; such a technique might be the best way to produce ions from refractory metals. Charge exchange can also be used,

particularly if the parent ion is easier to produce and isolate by direct ionization than the daughter ion (Itano and Wineland, 1981). More recently, highly stripped ions have been trapped as recoils from collisions of neutrals with high-energy, highly stripped ion beams (Vane *et al.*, 1981; Church, 1982). These experiments have so far dealt only with collision processes (electron capture), but the possibility of doing spectroscopy on high-Z ions is very exciting.

E. Ion Detection

Perhaps the most direct way to detect ion number is by ejection-counting methods (Dehmelt and Jefferts, 1962; Jefferts, 1968; Dawson and Whetten, 1968; Gräff *et al.*, 1980; Dawson, 1980). By driving the resonant motion of the ions, the resulting induced currents in the electrodes can be an effective way to monitor ion number (Fisher, 1959; Dehmelt, 1967; Dehmelt and Walls, 1968; Wineland and Dehmelt, 1975a; Blumberg *et al.*, 1978; McIver, 1978a,b; Van Dyck and Schwinberg, 1981a). This can be quite sensitive since a single electron or positron can be detected with good signal to noise ratio. In one case, H_2^+ "test" ions have been used to sample $^3He^+$ ion density by observation of their space-charge-shifted frequencies (Dehmelt, 1967; Schuessler *et al.*, 1969). Both the number and temperature of ions can be monitored with the "bolometric" technique (Dehmelt and Walls, 1968; Church and Dehmelt, 1969; Walls and Dunn, 1974; Wineland and Dehmelt, 1975a; see also Gaboriaud *et al.*, 1981), where one observes the mean square value of the induced currents in the electrodes. Induced charge frequency shifts (Wineland and Dehmelt, 1975a) might also be used to infer ion number. Observation of Doppler-induced (Schuessler, 1971b; Major and Werth, 1973; Major and Duchêne, 1975; Lakkaraju and Schuessler, 1982) or inhomogeneous magnetic field-induced sidebands on rf or microwave transitions can give information on cloud size and temperature. The use of laser-induced fluorescence techniques can be utilized to detect both ion cloud size and number as described previously. In the case of the Penning trap, the cloud density can be measured by observing the magnetron rotation-induced Doppler shift of the ion resonance lines (Bollinger and Wineland, 1983). The sensitivity of these fluorescence methods is indicated by the ability to detect single ions (Neuhauser *et al.*, 1980; Wineland and Itano, 1981; Nagourney *et al.*, 1983; Ruster *et al.*, 1983).

F. Polarization Production/Monitoring

Ion samples have been polarized using spin exchange with polarized neutral beams (Dehmelt, 1969; Gräff *et al.*, 1968, 1969, 1972; Church and

Mokri, 1971; Schuessler, 1979, 1980). Changes of polarization in these experiments have been detected by observing the heating due to spin-dependent inelastic collisions or by detecting spin-dependent ion neutralization by detecting ion number. Changes in polarization of trapped electrons have also been detected by observing changes in polarization of a transmitted atomic beam (Gräff and Holzscheiter, 1980) or by the kinetic energy dependence on polarization of electrons ejected into an inhomogeneous field (Kienow *et al.*, 1974; Gräff *et al.*, 1980). Optical-induced fluorescence techniques discussed below may be the dominant choice in future experiments on atomic ions; we recall, however, that the first optical techniques relied on orientation dependence of ion photodissociation (Dehmelt and Jefferts, 1962). More recently, orientation-dependent photodetachment has been used (Jopson and Larson, 1981).

G. Other Types of Traps

Variations on the types of traps discussed above have been considered. It is possible to use the Paul and Penning traps in a combined mode (Fisher, 1959; O and Schuessler, 1980b), but such traps have not really been used yet. Some rf traps with a "race track" design based on a closed-loop configuration for the Paul mass spectrometer have also been tested (Church, 1969). In addition, six-electrode rf traps with three-phase drive have also been demonstrated (Wuerker *et al.*, 1959b; Haught and Polk, 1966; Zaritskii *et al.*, 1971). For many years, trapped ion cyclotron resonance (ICR) spectrometers (McIver, 1970, 1978a,b; Comisarow, 1981) have been used by chemists; this configuration is basically a Penning trap with rectangular electrodes. (We note also that this is the typical configuration in a sputter ion pump.) Trap arrays (Major, 1977) have been proposed to increase overall trapping efficiency and variations on the Kingdon trap have also been proposed (McIlraith, 1971). Finally we note the possible use of "space charge" traps (Redhead, 1967; Hasted and Awad, 1972; Donets and Pikin, 1976; Hamdan *et al.*, 1978). Such devices have been mainly used in collision studies; for high-resolution spectroscopy the traps described above seem superior.

III. Lepton Spectroscopy

A. Historical Perspective

The only stable leptons that can take advantage of the long containment times possible in the Penning trap are the electron and the positron. Thus,

inspired by the early spin exchange, optical pumping experiments at the University of Washington (Dehmelt, 1956, 1958), these particles have subsequently been trapped and studied to high precision in a series of highly successful geonium experiments (Van Dyck, *et al.*, 1977, 1978; Schwinberg *et al.*, 1981a, 1981c, 1983). However, the first truly precise rf spectroscopy experiment, carried out on electrons in such a trap, was conducted by G. Gräff and associates in Bonn and Mainz, West Germany. The Penning trap was placed in the uniform magnetic field region of a standard atomic beam machine (Gräff *et al.*, 1968). A state-selected sodium beam interacts with the trapped electrons, causing the cloud to become polarized; subsequent spin-dependent energy-transfer collisions with the polarized atoms then lead to an observable change in the number of electrons remaining in the trap after a fixed interaction time. By applying a microwave field at the spin precession frequency ν_s and then an rf field at the spin-cyclotron difference frequency ν_a, the free electron g-factor was measured to a precision of 0.3 ppm (Gräff *et al.*, 1969):

$$g(e^-)/2 = 1.001,159,660(300) \tag{9}$$

This same experiment was subsequently modified to incorporate the non-destructive bolometric detection method discussed in Section II.E, thus yielding the g factor with approximately the same precision (see Church and Mokri, 1971). However, the potential for improvement was limited by relatively large linewidths attributable to relativistic kinematics, second-order Doppler effects, and possible magnetic field inhomogeneity over the large electron cloud. Another possible limitation to this work was the electrostatic cloud shifts associated with the ν_a resonance (see Wineland and Dehmelt, 1975c).

About this same time, a different technique for measuring the electron (or positron) g-factor had begun to show great promise at the University of Michigan under the guidance of H. R. Crane (see Wilkinson and Crane, 1963; Rich, 1968a,b). Referred to as the free precession method, the scheme directly observes the relative orientation between the precessing spin and the electron's orbital momentum after a fixed containment time in a weak magnetic mirror trap. This technique was dramatically refined by A. Rich and associates at Michigan (see Wesley and Rich, 1971), achieving a precision of 3 ppb in the electron's g-factor:

$$g(e^-)/2 = 1.001.159.657,700(3,500) \tag{10}$$

At this point, the precession method also found certain limitations such as finite observation time, relativistic mass corrections, possible space-charge shifts, and large containment volumes ($\approx 10^2$ cm^3 with corresponding

uncertainty in the magnetic field. This experiment is presently being rebuilt in hopes of achieving a precision of 0.010 ppb in the g-factor.

However, since 1959 H. Dehmelt and colleagues had been studying electron clouds in a Penning trap at very low pressures ($< 10^{-9}$ Pa or 10^{-11} Torr), cooled by coupling axially to a resonant tuned circuit. This early work established the basic nondestructive bolometric technique (Dehmelt and Walls, 1968) whereby either excitation of the cyclotron resonance or alternating excitation of spin and g-2 frequencies causes an increase in the monitored axial temperature. This bolometric scheme thus produced a g-factor measurement

$$g(e^-)/2 = 1.001,159,580(80) \tag{11}$$

whose precision appeared to be limited by electrostatic cloud perturbations (Walls, 1970; Walls and Stein, 1973). However, these initial Penning trap studies did point out the advantages of reducing the cloud to its ultimate irreducible size, i.e., a single electron, capable of being continuously observed for several days (Wineland *et al.*, 1973). This now set the stage for the geonium experiments carried out on single electrons (Section III.B) and single positrons (Section III,C) by one of the authors (RSV) in collaboration with P. Schwinberg and H. Dehmelt.

B. Electron Geonium Experiment

1. The Geonium Atom

The basic apparatus (Van Dyck, *et al.*, 1978) is shown schematically in Fig. 4. The electron's driven axial motion at $\nu_z \approx 60$ MHz induces a measurable voltage across the high-impedance tuned circuit. By keeping a large drive amplitude fixed and the frequency set for off-resonance excitation ($\delta\nu \approx 10$ kHz), the smallest unit of voltage is found (by loading different bunches of electrons) for which all other signals are integral multiples, thus signifying the presence of a single electron. This can also be verified by comparing respective linewidths. Now isolated from external perturbations within a relatively small volume ($< 3 \times 10^{-7}$ cm^3) at ultralow pressures, the trapped electron is bound via the trap's electrode structure and the magnet to the earth as if it were a mestastable pseudoatom. The University of Washington researchers therefore refer to this pseudoatom as "geonium." Further discussion of the geonium state can be found in a series of tutorial lectures (Dehmelt, 1983; Ekstrom and Wineland, 1980).

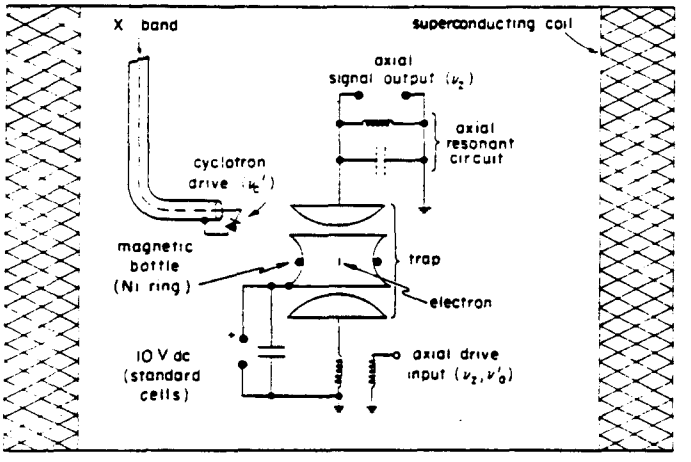

FIG. 4. Schematic of the geonium apparatus. Placed into the bore of a superconducting solenoid and operated at 4.2 K, the basic Penning trap is used to isolate single electrons and detect their driven axial motion via a resonant tuned circuit. Magnetic transitions are observed by coupling respective magnetic moments via the nickel ring to the precise axial resonance frequency. (From Van Dyck *et al.*, 1978.)

2. *Precision Axial Resonance Spectrometer*

Because of the need for holes and slits in the basic electrodes and the unavoidable truncation and machining imperfections of the surfaces, terms higher than quadratic appear in the potential distribution (see Section II). In order to compensate for these effects, guard rings are placed between the endcaps and ring and their potential is varied until the narrowest possible unshifted axial resonances are obtained, i.e., reduced 100-fold relative to those from uncompensated traps (Van Dyck *et al.*, 1976). The resulting single electron linewidth (shown in Fig. 5) is within 10% of the expected damping linewidth and the frequency resolution is approximately 10 ppb (for the signal-to-noise ratio as shown).

This narrow axial resonance is now used in a feedback detection circuit in which a very stable frequency synthesizer supplies the rf drive. Of the two quadrature components shown in Fig. 5, the dispersion-shaped curve yields the error signal, which is integrated to produce a correction that is added back to the ring in order to close the loop. In this way, the axial motion is locked to the synthesizer at ν_z and the correction signal is proportional to any shift $\delta\nu_z$. This type of nondestructive synchronous detection of a single electron (or ion) forms the precision axial-resonance spectrometer mode of operation.

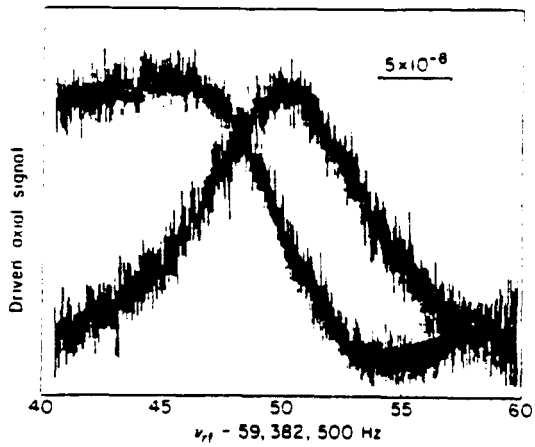

FIG. 5. Graph of the synchronously detected axial resonance. Linewidths of 8 Hz out of 60 MHz are achieved in a well-compensated Penning trap in a cryogenic (4.2 K) environment. Both the absorption and dispersion phases of the signal are given for this resonance using a 0.5-sec time constant. (From Van Dyck *et al.*, 1978.)

3. Magnetic Coupling

The electron's magnetic resonances have been indirectly observed by constructing a shallow magnetic bottle obtained from a small nickel ring located in the midplane of the ring electrode. The uniform axial field B is therefore modified (in cylindrical coordinates) to yield

$$B_z = B_0' + B_2(z^2 - r^2/2) \tag{12}$$

and

$$B_r = -B_2 rz$$

where B_2 is fixed at approximately 0.012 T/cm² (or 120 G/cm²) when the nickel ring is saturated. The weak interaction with the electron's magnetic moment yields an additional axial restoring force and the following axial frequency shift:

$$\delta\nu_z = \left(m + n + \frac{1}{2} + \frac{\nu_m}{\nu_c} q\right)\delta \tag{13}$$

where $\delta = \mu_B B_2/(2\pi^2 M\nu_z) \approx 1$ Hz and the integers m, n, and q are respectively spin, cyclotron, and magnetron quantum numbers. Thus, this coupling yields an occasional random jump in the $\delta\nu_z$ correction signal and a 1-Hz change in the resulting noise "floor" for each induced spin flip ($\Delta m = \pm 1$).

This same magnetic bottle is also used to generate the perpendicular rf field required to flip the electron's spin. As indicated by the radial field B_r in Eq. (12), an auxiliary axial drive at ν_a' combined with the cyclotron motion generates sidebands at $\nu_c' \pm \nu_a'$. Since by definition $\nu_a' \equiv \nu_z - \nu_c'$, it follows that ν_z is one of the rotating components.

4. *Sideband Cooling*

In order that the electron may be found reliably at the same radial position in time, it is centered at the top of the radial electric and magnetic hills by using a novel sideband cooling technique first developed at the University of Washington, in which an inhomogeneous electric field is applied at $\nu_z + \nu_m$ to the trapping volume (Van Dyck *et al.*, 1978; Wineland, 1979). The electron's magnetron motion in the inhomogeneous field generates a field component at ν_z which damps $h\nu_z$ quanta into the tuned circuit with the extra $h\nu_m$ quanta being absorbed into the magnetron motion, thereby shrinking r_m. Figure 6 strikingly confirms this process as the magnetic coupling is also used to monitor changes in the magnetron magnetic moment [see Eq. (13)]. Note that r_m grows exponentially when $\nu_z - \nu_m$ drive is applied. In addition, this sideband technique allows ν_m to be determined and, when compared to $\nu_z^2/2\nu_c'$, is found to agree within 100 ppm.

5. *Resonance Data*

As shown in Fig. 4, a small diode is used both as a frequency multiplier to generate the cyclotron drive and an antenna to launch microwaves into the

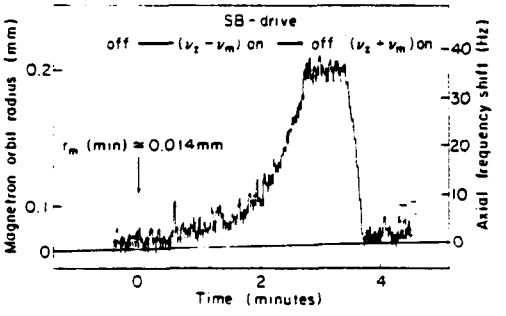

FIG. 6. Graph of changes in the magnetron orbit radius with time. The axial resonance spectrometer technique is used to observe changes in the magnetron radius by driving the axial motion on the $\nu_z \pm \nu_m$ sidebands. In this way, $h\nu_m$ quanta are absorbed (or emitted) in conserving total energy, thereby shrinking (or expanding) the magnetron orbit. (From Van Dyck *et al.*, 1978.)

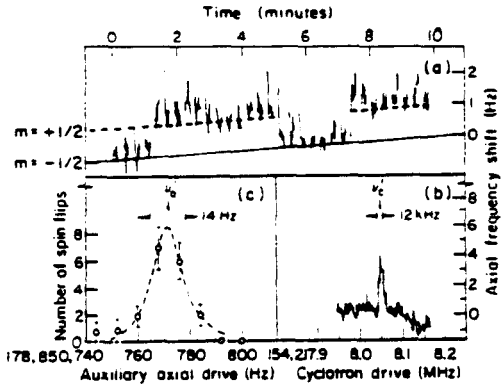

FIG. 7. Graph of electron geonium resonance data. The cyclotron resonance in (b) is measured at 5.5 T by detecting the corresponding axial frequency shifts while using a very low axial drive. The spin-flip data in (a) is obtained by alternating both a strong detection and auxiliary drives; the number of spin flips observed out of say 30 attempts for a fixed-frequency auxiliary drive is plotted in (c).

trap. Figure 7b shows a typical cyclotron resonance obtained at 5.5 T while using the lowest axial drive that still maintains axial lock. The interference between axial drive and thermal noise via the magnetic bottle makes such low drives necessary. Unfortunately, the signal-to-noise ratio for such drives is inadequate to observe the 1-Hz steps in the noise floor. Therefore, an alternating detection/drive scheme was used to obtain the spin flip data shown in Fig. 7a. For a fixed frequency of the auxiliary drive, the number of 1-Hz axial frequency steps produced out of say 30 attempts is counted and plotted versus frequency in order to yield an anomaly resonance typified by that in Fig. 7c; the resolution of this data is ≈ 40 ppb.

6. *Results and Conclusions*

The procedure for correcting the magnetic resonances for the presence of Penning trap electrodes is nearly invariant to small misalignments or asymmetries (Brown and Gabrielse, 1982). Thus, the electron's g-factor (or anomaly) is given to a precision greatly exceeding 10^{-12} by the following:

$$\frac{g(e^-)}{2} - 1 = a_e = \frac{\nu_a' - \nu_z^2/2\nu_c'}{\nu_c' + \nu_z^2/2\nu_c'} \tag{14}$$

where ν_a', ν_c', and ν_z must be the observed resonant frequencies. Presently, the measurement of ν_c' has not shown any systematic errors, but ν_a' has been found to show a small negative shift ($< 4 \times 10^{-8}$ for the full range of

anomaly powers used) that depends on the strength of the auxiliary drive. Though at present, no adequate explanation exists for this dependence, an extrapolation to zero amplitude has yielded consistent anomalies for three different magnetic field strengths: 1.8, 3.2, and 5.1 T. Various other small shifts are possible (see Van Dyck *et al.*, 1978; Dehmelt, 1981a, 1983), but at the present level of accuracy, none have been observed to affect the anomaly, either because they are too small or because they affect ν_c' and ν_a' in the same way. An extrapolated unweighted average of all runs (Van Dyck *et al.*, 1979) yields

$$g(e^-)/2 = 1.001,159,652,200(40) \tag{15}$$

which can be compared with the best theoretical prediction based on quantum electrodynamics (Kinoshita and Lindquist, 1981) and the e/h fine-structure constant α (Williams and Olsen, 1979):

$$g_{thy}/2 = 1.001,159,652,460(147) \tag{16}$$

Conversely, QED theory and the experimental g-factor predicts the fine-structure constant:

$$\alpha^{-1} = 137.035,993(10) \tag{17}$$

which agrees very well with the e/h determination of α:

$$\alpha^{-1} = 137.035,963(15) \tag{18}$$

In order to reach a g-factor precision of 1 part in 10^{12} in the future, a new bottleless Penning trap is being developed [see Dehmelt (1981a) for a possible bottleless detection scheme] which may utilize the relativistic mass shift associated with the cyclotron excitation (Gabrielse and Dehmelt, 1980). A new trap technology is being developed which uses copper electrodes with a split ring for direct production of the spin-flip field, mounted into an all-metal vacuum envelope with indium seals and nonmagnetic ceramic feedthroughs (Gabrielse and Dehmelt, 1983).

C. Positron Geonium Experiment

1. Preparing the Positron Geonium State

The primary technological difference between this and the electron geonium experiment is the continuous positron loading scheme (Schwinberg *et al.*, 1981c) which is completely static and relies upon radiation damping in a separate storage trap (see Fig. 8). A sealed ^{22}Na positron emitter, mounted off-axis (at $\frac{1}{4}r_0$), is biased in such a way that a trappable positron passing

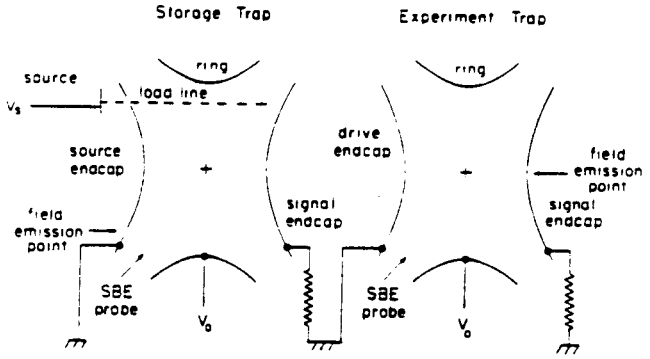

FIG. 8. Schematic of the double-trap configuration. The storage trap contains a sealed ^{22}Na positron emitter located at $\frac{1}{2}r_0$. SBE probes are used in the sideband cooling scheme to radially center the trapped positrons prior to transferring some of them into the highly compensated experiment trap. (From Schwinberg *et al.*, 1981a.)

through the source hole will have most of its energy ($\approx$ 100 keV) in the radial motion and will be temporarily trapped for one magnetron period, before returning to its original entry point. During this time, enough axial energy may be extracted by the damping circuit to permanently trap the positron and to subsequently thermalize its axial motion. In contrast, the relativistic cyclotron energy will damp quickly (a few seconds) by synchrotron radiation. Finally, the trapped positron is centered using the motional sideband technique described in Section III,B,4. A typical loading rate during early liquid helium operation at 5.1 T was 23 e^+/hr with a 0.5 mCi source within a 5-V deep storage trap (Schwinberg *et al.*, 1981c).

The carefully constructed compensated experiment trap (also shown in Fig. 8) was found to be necessary because the large off-axis holes, required for positron loading, prevent the storage trap from being fully compensated. Therefore, some of the centered positrons are moved into the experiment trap by pulsing the two adjacent endcaps down to the approximately common ring potential (-8 to -10 V) for a few microseconds. Once transferred, they are detected by using a large off-resonance axial drive similar to the loading drives described for electrons in Section III,B,1. After determining that more than one have been transferred, the excess are systematically ejected using intense rf pulses at $\nu_z + \nu_m$ on the enclosed side band excitation (SBE) probe. The pulse amplitude is carefully adjusted in order to require at least 10 consecutive pulses to eject an e^+ from the cloud. Once a positron is isolated, the axial drive is reduced in order to observe a 4-Hz axial resonance that is used in the precision axial spectrometer mode described in Section III,B,2.

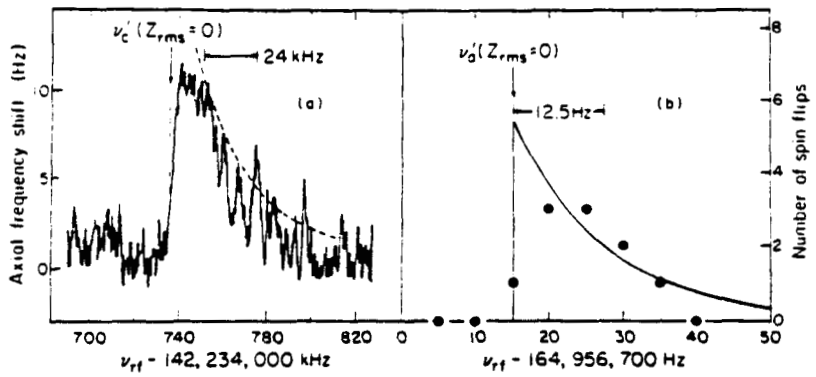

FIG. 9. Graph of the positron geonium resonance data. The cyclotron resonance in (a) has a lineshape characterized by a high-frequency exponential tail and a low-frequency edge (for $z_{rms} = 0$); the dotted curve is an exponential with a 24-kHz decay constant. The corresponding anomaly resonance in (b) is similar to the cyclotron resonance, but with an edge feature convolved with the relaxation rate for the axial resonance. The solid line in (b) represents the ideal lineshape with a 12.5-Hz decay constant. (From Schwinberg *et al.*, 1981a.)

2. *Measurements*

For this apparatus, the magnetic bottle produces a 1.3-Hz shift per unit change in the magnetic quantum level as described in Section III,B,3. Figure 9a shows a typical positron cyclotron resonance but now with sufficient resolution to observe a linewidth characterized by a high-frequency exponential tail due to the coupled thermal Boltzmann distribution of axial states. The dotted curve represents an exponential with a 24-kHz decay constant. However, this broad linewidth does not limit the resolution since it is the sharp low-frequency edge (for $z_{rms} = 0$) that corresponds to a cyclotron excitation at the bottom of the axial magnetic well. For this example, the field is resolvable to ≈ 10 ppb. Figure 9b shows the corresponding anomaly resonance taken upon alternating the detection and excitation (as explained in Section III,B,5). The characteristic shape is similar to that of the cyclotron resonance, though the edge feature is typically smeared by the relaxation rate of the axial states. Therefore, the precision of the anomaly edge feature, taken as the half linewidth, is ≈ 30 ppb.

3. *Results and Conclusions*

Time studies of the cyclotron resonances found an effective magnetic field jitter ($\approx \pm 25$ ppb over $\approx 10^2$ sec) which is believed to be due to collisions

with background gas varying the minimum radial position in the magnetic bottle. The source of this background was later traced to a small crack in the glass envelope. However, prior to rebuilding the positron apparatus, the only systematic effect observed was again the small negative shift proportional to the strength of the auxiliary axial drive ν_a'. From four initial positron runs, a preliminary positron g-factor (Schwinberg *et al.*, 1981a,b)

$$g(e^+)/2 = 1.001,159,652,222(50) \tag{19}$$

is obtained from a weighted least squares extrapolation using the systematic power dependence observed for the previous electron work. This result agrees well with the electron's g-factor [Eq. (15)] and the theoretical prediction [Eq. (16)]. It is also 20,000 times more precise than the only other direct measurement of the positron g-factor (Gilleland and Rich, 1972) using the Michigan free precession technique. Finally, by combining measured e^- and e^+ g-factors, the comparison

$$g(e^+)/g(e^-) = 1 + (22 \pm 64) \times 10^{-12} \tag{20}$$

may well represent the most severe symmetry test of charge conjugation-parity reversal – time reversal (CPT) invariance known to date. An excellent discussion of the discrete symmetries using free leptons can be found in a review by Field *et al.* (1979).

IV. Mass Spectroscopy

A. Introduction

Because of long containment times and small sample volumes, the Penning trap is an ideal device for measuring the mass of stable ions using ion cyclotron resonances. This can be compared to such devices as the resonance rf mass spectrometer of Smith and Wapstra (1975), which has demonstrated a resolution of 1 – 10 ppb by carefully controlling various systematic effects. In contrast, an ion cooled down in a Penning trap can be confined to such a small volume that both the electric and magnetic fields can be easily controlled by using small electric steering fields (Van Dyck *et al.*, 1980), guard electrodes for compensation, and magnetic shim coils for producing the required field symmetry and uniformity. Finally, refined rf techniques allow small numbers (≤ 10) of light ions (< 10 u) to be observed in such a trap, and weak self-contained sources can be used without appreciably altering the background pressure. Eventually, laser fluorescence tech-

niques may allow simple detection of single ion mass ratios by observing changes in fluorescence as the ion orbits are excited (Wineland *et al.*, 1983).

This section specifically describes direct precision measurements of the proton-to-electron mass ratio (m_p/m_e) using the Penning trap. However, variations of these same techniques could be used to measure any of the light ion masses (such as ^{3}H and ^{3}He) with an *in situ* field calibration obtained using either the electron or proton cyclotron resonance. Ultimately, these techniques may also be used to study more exotic species such as the antiproton (Dehmelt *et al.*, 1979; Torelli, 1980).

Presently, there are three direct measurements of m_p/m_e using the Penning trap to alternately confine both e^- and p^+: two at the University of Mainz and one at the University of Washington.

B. First Mainz Experiment

This experiment by Gärtner and Klempt (1978) has a thermionically produced electron beam which ionizes background hydrogen gas, obtained from a palladium leak, to produce secondary electrons, H^+, and H_2^+ in the trapping volume. A pressure of 10^{-7} Pa (or 10^{-9} Torr) then yields storage times of ≈ 60 sec for protons and ≈ 60 min for electrons. Typically, a few thousand ions would be trapped and detected via their axial motion interacting with a tuned circuit across the endcaps. By sweeping the dc ring voltage V_0, the axial resonance at ν_z can be made to coincide with the frequency of the tuned circuit, thus yielding a detectable decrease in signal as

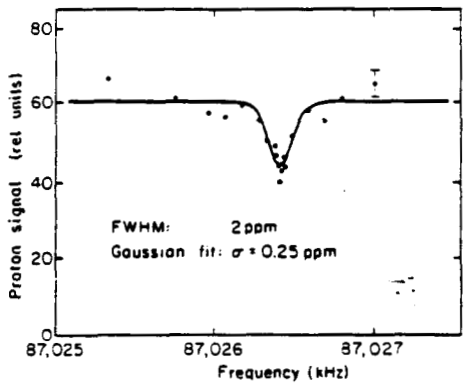

FIG. 10. Graph of the proton cyclotron resonance. The final average number of trapped protons is plotted versus frequency for the case of $V_0 = 20$ V. Resonance is indicated by an $\approx 25\%$ decrease in the number of protons remaining in the trap per cycle after the rf drive is applied, and the solid line is a Gaussian line fit with a 0.25 ppm statistical uncertainty in $\nu_z(p^+)$. (From Gärtner and Klempt, 1978.)

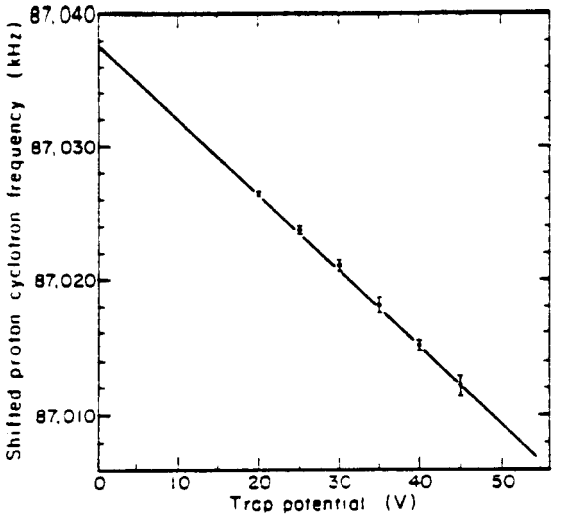

FIG. 11. Graph of the proton cyclotron frequency versus the trapping potential. The bolometrically measured $\nu_c'(p^+)$ has been corrected for various small systematic effects such as space charge and field inhomogeneity shifts. The straight line represents a linear least squares fit that is extrapolated to zero in order to yield $\nu_c(p^+)$. (From Gärtner and Klempt, 1978.)

the ions short out the noise coming from the tuned circuit. The width of the resulting notch can be used to estimate the number of trapped ions (Wineland and Dehmelt, 1975a).

A complete detection cycle begins with a pulse of electrons to load the ions, followed by a storage time for cooling the motion, an interaction time when rf fields are applied, a linear sweep of V_0 to detect the ions, and a final electric pulse to clear the trap. Excitation of the cyclotron resonance produces an increase in cloud temperature and an enhanced loss of trapped ions. A typical example of a proton cyclotron resonance is shown in Fig. 10. Each point represents the number of remaining protons per cycle averaged over many complete cycles at each frequency setting. A typical 2-ppm linewidth could be statistically resolved to 0.25 ppm, but the final error is increased by 10 because of such systematic effects as the uncertainty in the electric field strength, inhomogeneity and decay in time of the magnetic field, and space-charge broadening and shifting of the cyclotron resonances in an imperfect Penning trap.

From Section II.B, the trapping electric field shifts the cyclotron frequency as follows:

$$\nu_c' = \nu_c + cV_0/[\pi(r_0^2 + 2z_0^2)B_0] \tag{21}$$

Thus, the extrapolation to zero potential as shown in Fig. 11 yields the

unshifted frequency $\nu_c(p^+)$ with a combined uncertainty of 2.6 ppm. However, because of its much greater frequency (160 GHz), the electron's cyclotron frequency is much less affected by space-charge effects and residual anharmonicity. But in this case, relativistic shifts due to the increased energy of the stored electrons contribute greatly to the 1.3-ppm uncertainty in $\nu_c(e^-)$; thus, the final mass ratio is

$$m_p/m_e = 1836.15020(530) \tag{22}$$

C. Second Mainz Experiment

This experiment (by Gräff *et al.*, 1980, 1983) has a compensated copper Penning trap with the central ring electrode split parallel to the z axis in order to apply an rf electric field normal to the axial magnetic field. The trap is installed in one end of a 37-cm-long copper drift tube which extends well out of a superconducting solenoid. A channel plate detector is mounted at the receiving end of the drift tube to count ions (or electrons) versus their arrival time at the detector. The entire apparatus is mounted horizontally into the bore of a 6.4-T shimmed superconducting magnet.

Unlike the previous Mainz research in which ν_c' is measured versus V_0, this experiment uses a direct induction of the transition at ν_c (i.e., $\nu_c' + \nu_m$) applied at low electric field strengths. The experimental procedure begins by pulsing thermionic electrons for ≈ 100 msec to produce either trapped electrons or protons. During the following 1 sec, the ring–endcap potential is ramped down to 1 V and (for the proton case) an axial drive is simultaneously applied to sweep out all extraneous ions such as H_2^+, H_3^+, and He^+. The cyclotron frequency ν_c is then applied for ≈ 500 msec, after which the trap is cleared by a linear voltage sweep with a superimposed sequence of pulses that define the starting time of the ejected particles and start a set of fast counters which accumulate data to generate the time-of-flight spectrum.

The flight time of the moving charge is determined by its initial kinetic energy along the z axis and by the size of its magnetic moment. In other words, when the rf field is resonant at ν_c, the transverse orbit increases, resulting in the greater acceleration of the charge in the inhomogeneous field along the drift tube axis; the corresponding reduction in the proton's average time of flight is shown in Fig. 12. Note that the mean flight time ($\approx 30\ \mu$sec) is reduced by several percent and the linewidth (FWHM) is 0.3 ppm. Similar plots were obtained for the electron case, but with a typical average flight time of 3 μsec and a linewidth of 0.4 ppm.

The largest proton systematic effect is shown in Fig. 13, where ν_c is plotted versus the number of trapped ions (and extrapolated to zero). However, for

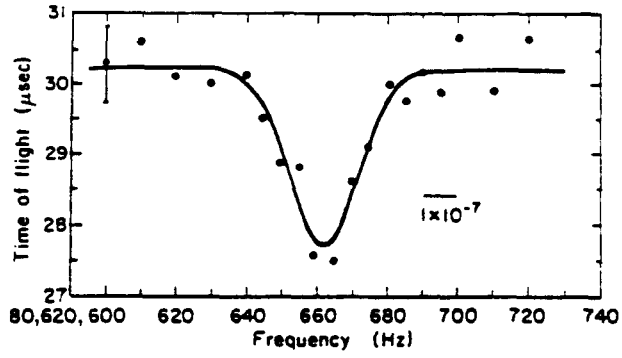

FIG. 12. Graph of the proton cyclotron resonance. The protons' time of flight is plotted as a function of the frequency of the rf drive applied prior to ejection from the Penning trap. The solid curve represents a fit to a Gaussian distribution. (From Gräff *et al.*, 1980.)

the electron the absorbed microwave power produces a sizeable relativistic mass increase, and thus a shift and broadening of the ν_c resonance. Since the lineshape could not be explained theoretically, half the FWHM linewidth is taken as the experimental uncertainty. The experiment was also performed at two different magnetic fields, 5.28 and 5.81 T, and the resulting mass ratios (which agreed within their statistical errors) were averaged to yield

$$m_p/m_e = 1836.15270(110) \tag{23}$$

This result agrees well with the first Mainz experiment and the previous least squares adjusted value (Taylor, 1976; Phillips *et al.*, 1977):

$$m_p/m_e = 1836.15165(68) \tag{24}$$

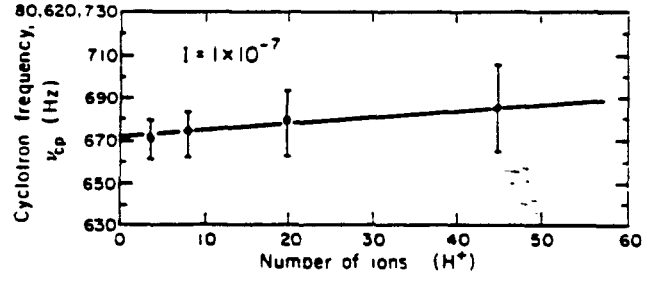

FIG. 13. Graph of the proton cyclotron frequency versus the number of trapped protons. Error bars correspond to $\nu_c(p^+)$ linewidths at FWHM and the relative slope of the dependence is -4.0×10^{-9}/ion. (From Gräff *et al.*, 1980.)

D. University of Washington Experiment

1. Experimental Method

This experiment by Van Dyck and Schwinberg (1981a, 1983) utilizes a somewhat smaller Penning trap than either Mainz experiment since a smaller size is more favorable (i.e., faster response time) for the synchronous detection scheme discussed in Section III,B,2. The trap contains a field emission point as an electron source, magnetic rings in each endcap for generating the axial magnetic coupling, and a hydrated titanium filament as a hydrogen source.

The fundamental experimental method also differs from the Mainz experiments in that the unperturbed cyclotron frequency ν_c is obtained by combining the three actual observed resonant frequencies $\bar{\nu}_c'$, $\bar{\nu}_z$, and $\bar{\nu}_m$ [where the bars allow for small perturbations; see Brown and Gabrielse (1982)]:

$$\nu_c^2 = \bar{\nu}_c'^2 + \bar{\nu}_z^2 + \bar{\nu}_m^2 \tag{25}$$

This is equivalent to Eq. (5b) in the limit of negligible imperfections and misalignments. The perturbed frequencies are then observed using at least one of three tuned preamplifiers: one on each endcap for axial detection [$\nu_z(e^-) \approx 136$ MHz and $\nu_z(p^+) \approx 10$ MHz] and one on the ring electrode split into four equal quadrants. This four-part "quadring" design allows the proton's cyclotron resonance to be excited by a balanced drive applied on two opposite quadrants and detected on the other pair externally tuned to the proton's cyclotron resonance at $\nu_c'(p^+) = 76.4$ MHz.

2. Measurements

With a 2.5-V well depth, the quadring trap could be adequately compensated in order to observe a single electron with a tuned circuit damping linewidth of ≈ 10 Hz (out of 136 MHz). The corresponding cyclotron resonance for this electron has a magnetic bottle-induced linewidth of 20–30 ppb and a low-frequency edge with resolution of 3 ppb (typical of that shown in Fig. 9a). With a well depth of -26 V, small numbers (<40) of protons can also be trapped and synchronously detected to yield very narrow ($\leqslant 0.2$ Hz) cyclotron resonances (see Fig. 14). In fact, on one occasion a reproducible linewidth of 0.03 Hz was observed to yield a precision greater than 0.5 ppb. The synchronously detected axial resonances have ≈ 50 times less resolution, but their relative contribution to the accuracy of $\nu_c(p^+)$ is only 2% via the magnetron (or correction) frequency.

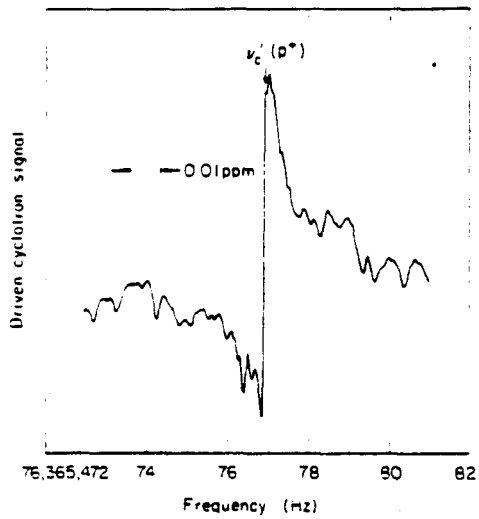

FIG. 14. Graph of the proton cyclotron resonance. This narrow dispersion-shaped curve is the result of direct synchronous detection of the resonance at $\nu_c'(p^+) = 76{,}365{,}476.9$ Hz using the split quadring design in a well-compensated Penning trap (for $V_0 = 54.4$ V). The linewidth, limited primarily by observation time, represents fewer than 40 protons. (From Van Dyck and Schwinberg, 1981a.)

3. *Results*

In order to eliminate the effects of space-charge fields upon the ion cloud cyclotron resonance (see Wineland and Dehmelt, 1975c), dissimilar ions are selectively removed using strong rf drives at their characteristic axial frequencies. However, this does not eliminate the dependence on the number of trapped ions in an imperfect Penning trap (Van Dyck and Schwinberg, 1983; Liebes and Franken, 1959). Since $\nu_c(e^-)$ was conveniently measured in preliminary work using small electron clouds ($< 50\ e^-$) and did not exhibit a number dependence, the mass ratio $m_p/m_e = \nu_c(e^-)/\nu_c(p^+)$, plotted in Fig. 15, reflects only the number dependence of $\nu_c(p^+)$. A linear fit of this data finds a relative slope of -1.2×10^{-10}/ion. This can be compared with -4.0×10^{-9}/ion found in the second Mainz experiment and $+1.1 \times 10^{-8}$/ion produced by an earlier uncompensated quadring trap.

The intercept of the linear fit in Fig. 15 corresponds to the preliminary mass ratio $m_p/m_e = 1836.15300(7)$. However, an analysis of bottle-related position dependence of the magnetic field suggests that a systematic error as large as 0.1 ppm may exist if the two charge types do not have the same average position in space. Thus, a preliminary mass ratio (Van Dyck and

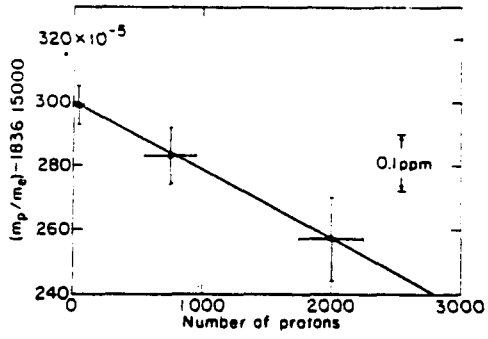

FIG. 15. Graph of the mass ratio versus the proton number. This dependence follows from the sensitivity of $\nu_c(p^+)$ to the number of trapped protons. The vertical and horizontal error bars are determined primarily by the $\nu_c(e^-)$ linewidth and the axial proton number calibration, respectively; the relative slope of the dependence is -1.2×10^{-10}/ion. (From Van Dyck and Schwinberg, 1981a.)

Schwinberg, 1981b) of

$$m_p/m_e = 1836.15300(25) \tag{26}$$

reflects the location uncertainty in the magnetic field. This systematic effect can be carefully checked in future experiments by directly varying the magnetic bottle strength B_2.

V. Atomic and Molecular Ion Spectroscopy

A. Optical Atomic Ion Spectroscopy

Relatively little optical spectroscopy has been performed on stored atomic ions, even though laser-induced fluorescence (LIF) provides a very sensitive detection method. Probably, this is due to the fact that few ionic resonance lines lie in the visible region of the spectrum, where tunable lasers are available.

Fluorescence of Ba^+ ions stored in rf traps has been observed, using a hollow cathode lamp (Duchêne *et al.*, 1977) or a dye laser (Iffländer and Werth, 1977a) as a light source. The hyperfine splitting of the 493-nm D_1 line of $^{137}Ba^+$ was observed by Blatt *et al.* (1979). The absolute wavelength (Drullinger *et al.*, 1980; Nagourney and Dehmelt, 1981a,b) and isotope and hyperfine splittings (Drullinger *et al.*, 1980) of the 280-nm D_2 line of Mg^+ have been measured, using frequency-doubled dye lasers. A saturation dip

in the 493-nm Ba^+ line was observed by Iffländer and Werth (1977b), showing that Doppler-free optical spectroscopy of ions is possible. Prior and Knight (1980) have observed hysteresis and line-narrowing effects due to hyperfine optical pumping in the LIF spectrum of metastable Li^+ in an rf trap. As discussed in Section II, optical excitation of ions has been used as a probe to measure ion cloud spatial distributions (Knight and Prior, 1979; Schaaf *et al.*, 1981), ion trapping efficiencies (Iffländer and Werth, 1977a; Plumelle *et al.*, 1980; Blatt *et al.*, 1979), lifetimes of metastable levels (Schneider and Werth, 1979; Knight and Prior, 1980; Plumelle *et al.*, 1980), and decay branching ratios (Osipowicz and Werth, 1981).

B. Laser Cooling

Laser cooling (also called optical sideband cooling or radiation-pressure cooling) was first proposed for trapped ions by Wineland and Dehmelt (1975b) and for free atoms by Hänsch and Schawlow (1975). This is a method by which a beam of light can be used to damp the velocity of an atom or ion. Thus, it is useful for reducing the second-order Doppler (time dilation) shift and first-order Doppler broadening of resonance lines. Most theoretical treatments of laser cooling of stored ions assume a harmonic trapping potential, a case which is approximated by the rf trap (Neuhauser *et al.*, 1980; Wineland and Itano, 1979; Javanainen and Stenholm, 1980, 1981a,b; Javanainen, 1980, 1981a,b; André *et al.*, 1981; Itano and Wineland, 1982). Itano and Wineland (1982) treat laser cooling in a Penning trap.

A harmonically bound ion can be cooled by a monochromatic laser beam tuned slightly lower in frequency than a strong resonance transition. For the usual experimental case, in which the natural linewidth of the transition is much greater than the ion's frequencies of motion, the process can be described as follows: When the velocity of the ion is directed against the laser beam, the light frequency in the ion's frame is Doppler-shifted closer to resonance, so that light scattering takes place at an increased rate. Since the photons are emitted in random directions, the net effect is to slow the ion down, due to the absorption of photon momentum. When the velocity of the ion is directed along the laser beam, the light frequency is shifted farther from resonance, so that it scatters photons at a reduced rate. The net effect, over a motional cycle, is to damp the ion's velocity. If the laser is tuned above resonance, it causes heating. The minimum number of scattering events required to cool an ion substantially, starting from 300 K, is on the order of 10^4, which is the ratio of the ion's momentum to the photon's momentum. When the transition linewidth is larger than the motional frequencies the lowest temperature that can be achieved is on the order of

$\frac{1}{2}\hbar\gamma/k_B$, where γ is the natural linewidth in angular frequency units. Typically, this is on the order of 0.1 to 1 mK. This limit is the result of a balance between the average damping force just described and heating due to fluctuations in the force, caused by the discreteness of the momentum transfers in the photon scattering events. Other cases have been treated theoretically. If the natural linewidth of the transition is less than the frequencies of motion, laser cooling is analogous to motional side-band cooling of the magnetron mode, as described for electrons in Section III.

Laser cooling of the cyclotron and axial modes of an ion in a Penning trap works in the same way as in a harmonic trap, for the case where the natural linewidth is much greater than any of the frequencies of motion. However, cooling of the magnetron mode requires that the momentum transfers take place preferentially in the same direction as the magnetron velocity (Wineland *et al.*, 1978). This can be arranged by focusing the laser beam so that it is more intense on the side of the trap axis on which the magnetron velocity is directed along the direction of light propagation. Simultaneous cooling of all three modes is possible with the proper frequency detuning, orientation, and intensity profile of the laser beam (Itano and Wineland, 1982). The minimum temperature is again about $\frac{1}{2}\hbar\gamma/k_B$.

Laser cooling of stored ions has been achieved by groups at Heidelberg and Boulder and more recently at Seattle (Nagourney *et al.*, 1983). The Heidelberg group has cooled Ba^+ in an rf trap using a cw dye laser tuned to the 493-nm D_1 resonance line (Neuhauser *et al.*, 1978a, b, 1980). Ions excited to the $6\,^2P_{1/2}$ level can decay to the $5\,^2D_{3/2}$ metastable level as well as to the ground state. In order to provide continuous laser cooling, a second cw dye laser at 650 nm was used to transfer ions in the $5\,^2D_{3/2}$ level back to the $6\,^2P_{1/2}$ level, from which they could decay back to the ground state. Small numbers of ions (down to one ion) were observed visually and photographically, through a microscope, by LIF. Figure 16 is a photograph of a single ion from these experiments. The image of a single ion, after deconvolution of instrumental effects, was determined to be about 0.2 μm in diameter, implying a temperature on the order of 36 mK. The $6\,^2S_{1/2}$–$6\,^2P_{1/2}$–$5\,^2D_{3/2}$ stimulated Raman resonance on a single ion has been observed by scanning the 650-nm laser, while keeping the 493-nm laser fixed (Neuhauser *et al.*, 1981; Dehmelt, 1982). This resonance is potentially very sharp, because the lifetime of the metastable level is 17.5 sec (Schneider and Werth, 1979). The rf trap used for the single-ion experiments was extremely small, with a separation between endcap electrodes $2z_0 \cong 0.5$ mm, in order to provide strong confinement. This makes it easier to satisfy the Dicke criterion (confinement to dimensions less than the wavelength), which makes the first-order Doppler broadening disappear (Dicke, 1953).

The Boulder group has cooled Mg^+ (Wineland *et al.*, 1978; Drullinger *et*

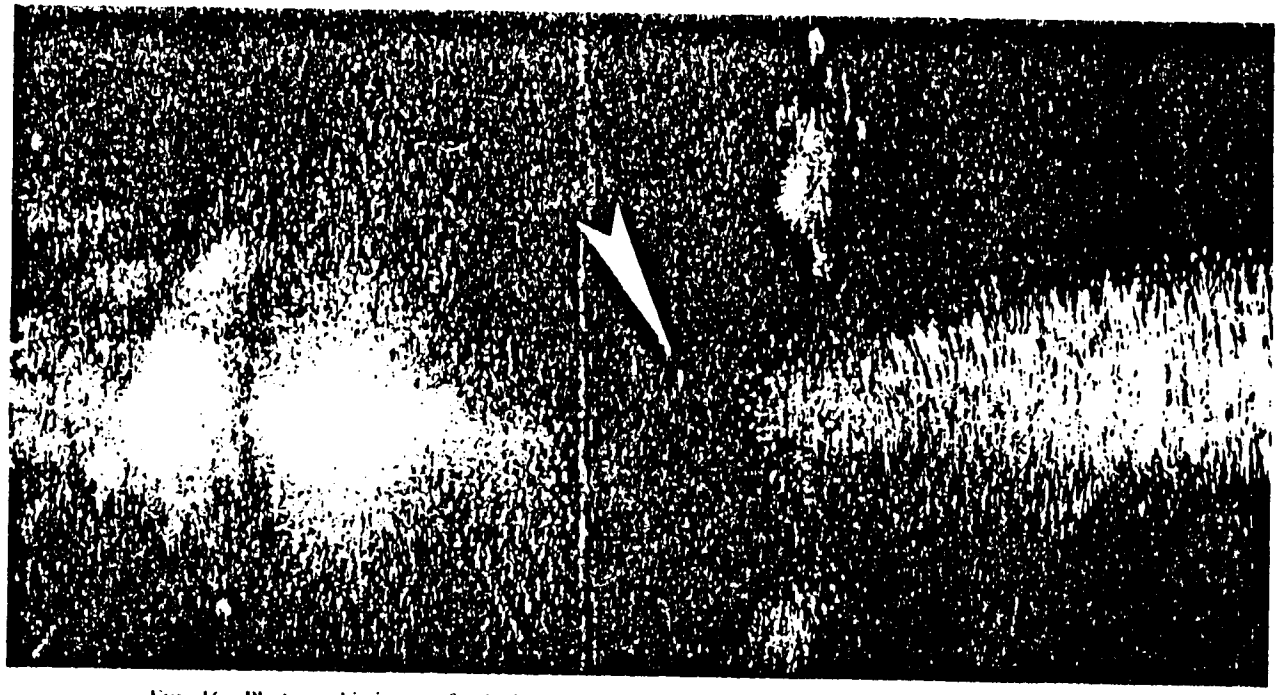

FIG. 16. Photographic image of a single Ba^+ ion (indicated by arrow) localized at the center of an rf trap.

al., 1980; Wineland and Itano, 1981) and Be^+ (Wineland and Itano, 1982), stored in Penning traps. The D_2 resonance lines at 280 nm and 313 nm for Mg^+ and Be^+, respectively, were used to provide cooling. The UV radiation was generated by frequency doubling the outputs of cw dye lasers in nonlinear crystals. The UV power was typically on the order of 10 μW. These ions can each be cooled using only one laser frequency, unlike Ba^+, because of the absence of intermediate metastable levels. The primary advantage of the Penning trap over the rf trap is the absence of rf heating, so that a cloud of ions can be cooled, even with a low-power source. (For a single ion, rf heating is not as severe a problem.) For some spectroscopic applications, the magnetic field required for operation of the Penning trap may be a disadvantage. Also, because of practical limitations on the magnitude of the magnetic field which can be applied, satisfying the Dicke criterion with a cooled ion is more difficult than with an rf trap.

The first observation of laser cooling of Mg^+ ions was made by monitoring the power of the currents induced by the thermal motions of the ions at the axial frequency (the bolometric technique discussed in Section II). For a fixed number of ions, this power is proportional to the temperature. The temperature was observed to decrease when the ions were illuminated by light tuned below the resonance frequency and to increase when the light was tuned above resonance, clearly demonstrating the laser cooling and heating effects (Wineland *et al.*, 1978). In later experiments, the resonance fluorescence photons emitted by the Mg^+ ions were counted by a photomultiplier tube. The measurement of the Doppler widths of the resonance curves, obtained by scanning the laser, indicated that the temperature of the ion cloud was below 0.5 K (Drullinger *et al.*, 1980).

It is easier to achieve very low temperatures with small numbers of ions, because space charge increases the radial electric field, which increases the magnetron velocity. In the limit of a single ion, this effect is absent. In order to achieve the lowest possible temperatures, experiments were performed on single ions (Wineland and Itano, 1981). In Fig. 17, the detected fluorescence intensity from a small cloud of $^{24}Mg^+$ ions is shown as a function of time. The three step-decreases are due to the loss of individual $^{24}Mg^+$ ions by charge exchange with ^{25}Mg atoms coming from an oven. The last plateau above background is due to a single, isolated ion. Optical Doppler width measurements showed that the combined cyclotron and magnetron temperature was 50 ± 30 mK. The axial motion was not cooled as efficiently, because the direction of propagation of the light beam was nearly perpendicular to the z axis. The axial temperature was estimated to be about 600 mK from a measurement of the extent of the axial excursions. Preliminary, unpublished results on clouds of Be^+ ions indicate that cyclotron–magne-

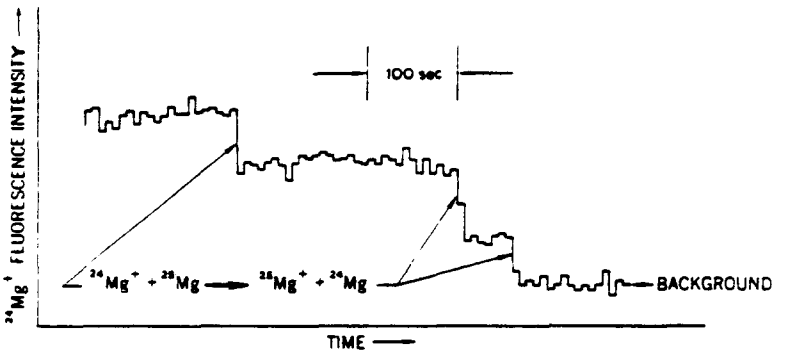

FIG. 17. Graph of the fluorescence from a small cloud of $^{24}Mg^+$ ions. The three large steps are due to the loss of individual ions. The last plateau above background is the fluorescence from a single ion. (From Wineland and Itano, 1981.)

tron temperatures less than 100 mK have been achieved (Bollinger and Wineland, 1983).

C. Microwave and rf Atomic Ion Spectroscopy

Observation of microwave or rf resonance transitions by absorption of the radiation is not generally feasible because of the small number of stored ions, so more sensitive detection methods have to be devised. The general scheme of all such methods includes three steps: (1) creation of a population difference between two states, (2) transfer of population from the greater to the lesser populated state by resonant radiation, and (3) detection of the population transfer.

In the ion storage exchange collision (ISEC) method, collisions with polarized atoms are used to carry out steps (1) and (3). Dehmelt and Major (1962) detected the rf Zeeman resonance of $^4He^+$ ions stored in an rf trap. The ions were polarized by spin-exchange collisions with a beam of Cs atoms, which were polarized by irradiation with circularly polarized resonance light. A change of the He^+ polarization, induced by resonant rf, was detected by a change of the number of ions remaining in the trap, due to spin-dependent charge-exchange collisions with the same atomic beam. The method was later used to observe hyperfine transitions in ground-state $^3He^+$, with linewidths as small as 10 Hz (Fortson *et al.*, 1966; Major and Dehmelt, 1968; Schuessler *et al.*, 1969). Auxiliary rf fields were required in order to make transitions which did not change the average electron spin polarization detectable. The zero-field hyperfine separation $\Delta\nu_1$ was determined to be 8,665,649,867(10) Hz.

Prior and Wang (1977) have measured the zero-field hyperfine splitting in the metastable 2s level of $^3He^+$, $\Delta\nu_2$, obtaining a value of 1,083,354,980.7(8.8) Hz. The ions were stored in a Kingdon trap. The population difference was created by using an auxiliary microwave field to drive ions in one hyperfine state to the $2\,^2P_{1/2}$ level, which decayed immediately. The hyperfine transition was then driven, and ions which made the transition were detected by counting the Lyman α decay photons when the auxiliary microwave field was applied again. The quantity $D_{21} = (8\Delta\nu_2 - \Delta\nu_1)$, obtained from these two ion storage experiments, is of interest as a test of quantum electrodynamic calculations, because it is largely free of nuclear structure corrections.

Optical-pumping double-resonance methods, in which population differences are created by illumination with resonance light and transitions are detected by changes in the absorption or fluorescence of the light, have been used previously on many neutral and charged atomic systems. Major and Werth (1973, 1978) were the first to apply this method to ion storage spectroscopy, in a measurement of the ground-state hyperfine structure of $^{199}Hg^+$ ions in an rf trap. A $^{202}Hg^+$ 194-nm D_1 resonance lamp was used to optically pump the $^{199}Hg^+$ ions into the $F = 0$ hyperfine state, because its spectrum strongly overlapped the $^{199}Hg^+$ D_1 resonance transition from the $F = 1$ state. The hyperfine resonance was detected by an increase in the fluorescence intensity. Work on this system has continued, because of its possible use as a frequency standard (Schuessler, 1971a; McGuire *et al.*, 1978; Jardino and Desaintfuscien, 1980; Jardino *et al.*, 1981a,b; Cutler *et al.*, 1982; Maleki, 1982). The most recent determination of the zero-field frequency is $\Delta\nu = 40{,}507{,}347{,}996.9(0.3)$ Hz (Cutler *et al.*, 1982).

Recently, optical pumping experiments on stored ions have been performed using tunable lasers as light sources. The ground-state hyperfine splittings of $^{137}Ba^+$ (Blatt and Werth, 1982), $^{135}Ba^+$ (Becker *et al.*, 1981), and $^{171}Yb^+$ (Blatt *et al.*, 1982) have been measured, using pulsed dye lasers and rf traps. The results were $\Delta\nu(^{137}Ba^+) = 8{,}037{,}741{,}667.69(0.37)$ Hz, $\Delta\nu(^{135}Ba^+) = 7{,}183{,}340{,}234.35(0.47)$ Hz, and $\Delta\nu(^{171}Yb^+) = 12{,}642{,}812{,}124.2(1.4)$ Hz. Microwave resonances as narrow as 60 mHz were observed in $^{171}Yb^+$ (see Fig. 18). This has a line Q (resonance frequency divided by FWHM) of 2×10^{11}. In some cases, optical pumping out of the absorbing ground state prevents use of the double-resonance method. This problem may be overcome, however, with the use of collisional relaxation (Blatt and Werth, 1982; Ruster *et al.*, 1983).

Microwave and rf transitions in laser-cooled Mg^+ (Wineland *et al.*, 1980; Itano and Wineland, 1981) and Be^+ (Wineland and Itano, 1982) stored in Penning traps have been observed by optical-pumping, double-resonance techniques. Laser cooling greatly reduces the second-order Doppler shift,

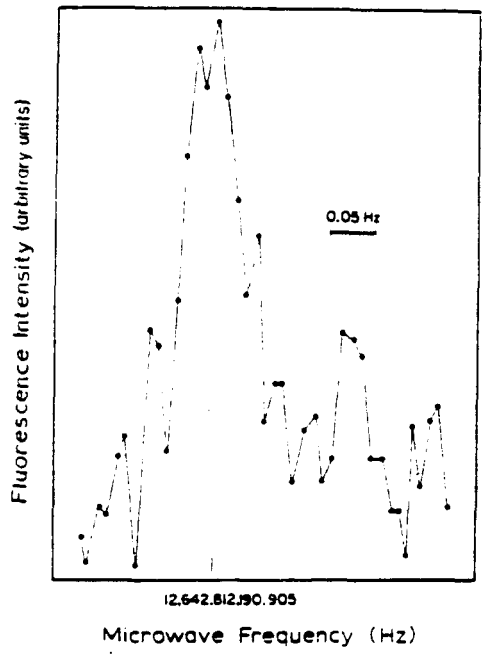

FIG. 18. Graph of the hyperfine resonance of trapped $^{171}Yb^+$ ions. The line Q is 2×10^{11}. (From Blatt *et al.*, 1982.)

which is a major source of uncertainty in other high-resolution stored-ion spectroscopic measurements. The optical pumping process is somewhat unusual in that population is transferred *into* the ground-state sublevel which is coupled most strongly to the excited state by the laser. A transition from this sublevel to another causes a temporary decrease in the fluorescence level. Since the number of photons *not* scattered during the time it takes the laser to pump an ion back into its original sublevel can be much greater than one, transitions can be detected with almost 100% efficiency (Wineland *et al.*, 1980). Electronic spin reorientation transitions in $^{24}Mg^+$ and both electronic and nuclear spin reorientation transitions in $^{25}Mg^+$ were observed. Auxiliary rf fields were required in order to make some of the transitions observable. At a magnetic field near 1.24 T, the first derivative of the $(M_I = -\frac{1}{2}, M_J = \frac{1}{2})$ to $(M_I = -\frac{1}{2}, M_J = \frac{1}{2})$ transition goes to zero. The resonance shown in Fig. 19 was obtained at that field and has a linewidth of only 12 mHz. The oscillatory lineshape results from the use of the Ramsey interference technique (Ramsey, 1956), applied in the time domain. Two coherent rf pulses, 1.02 sec long and separated by 41.4 sec, were applied. By fitting resonance frequencies to the Breit–Rabi formula, values were ob-

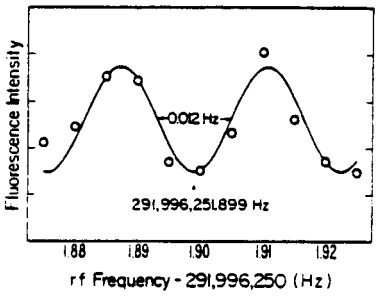

FIG. 19. Graph of the hyperfine resonance of trapped $^{25}Mg^+$ ions. The oscillatory lineshape results from the use of the Ramsey resonance method, implemented by applying two coherent rf pulses 1.02 sec long, separated by 41.4 sec. The solid curve is a theoretical lineshape. (From Itano and Wineland, 1981.)

tained for the hyperfine constant [$A = -596{,}254{,}376(54)$ Hz] and the nuclear to electronic g-factor ratio ($g_I/g_J = 9.299{,}484(75) \times 10^{-5}$). The uncertainties could be greatly reduced by observing another field-independent transition. Similar spectroscopy was performed on $^9Be^+$. Two field-independent transitions have been observed: ($M_I = \frac{1}{2}$, $M_J = -\frac{1}{2}$) to ($M_I = \frac{1}{2}$, $M_J = -\frac{1}{2}$,) at 0.68 T and ($M_I = -\frac{1}{2}$, $M_J = \frac{1}{2}$) to ($M_I = -\frac{1}{2}$, $M_J = \frac{1}{2}$) at 0.82 T. The magnetic field was calibrated by observing the cyclotron resonance of electrons which were trapped alternately in the same apparatus as the ions. Preliminary values for the ground-state constants are $A = -625{,}008{,}837.048(10)$ Hz, $g_I/g_J = 2.134{,}779{,}853(2) \times 10^{-4}$, and $g_J = 2.002{,}263(6)$. A $^9Be^+$ Ramsey resonance curve is shown in Fig. 20. The rf pulses were 2 sec long and were separated by 4 sec.

Gräff (1982) has proposed a method of observing parity- and time reversal-violating interactions by driving nuclear spin reorientation transitions in stored atomic ions, using rf electric and magnetic fields of the same fre-

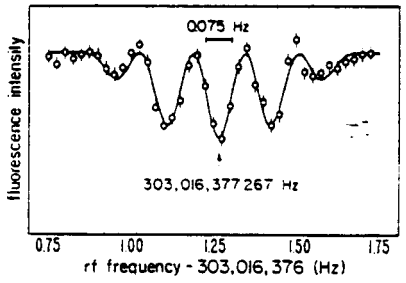

FIG. 20. Graph of the hyperfine resonance of trapped $^9Be^+$ ions, obtained by the Ramsey method. Two 2-sec rf pulses, separated by 4 sec, were used. The solid curve is a least squares fit to the theoretical lineshape.

quency but different relative phases. The method is particularly sensitive to the nuclear spin-dependent part of the parity-violating weak neutral current interaction, which has not yet been observed in atomic systems. Relative to atomic beam methods, the stored ion method has the advantage of longer coherent interaction times and the disadvantage of lower signal-to-noise ratio.

D. Application to Frequency Standards

The use of microwave or optical transitions of stored atomic ions in frequency standards has the combined advantages of long coherent interaction times (hence narrow linewidths) and small perturbations. The main disadvantage is the low signal-to-noise ratio due to the small number of ions that can be stored.

Work on frequency standards based on the 40.5-GHz hyperfine transition of $^{199}Hg^+$ ions has already been mentioned. The use of a field-independent transition in laser-cooled $^{201}Hg^+$ ions stored in a Penning trap has been proposed for a primary microwave frequency standard (Wineland *et al.*, 1981a). For microwave frequency standards, it may be particularly desirable to use a large number of ions in order to increase the signal-to-noise ratio. Therefore, the largest systematic frequency shift may be due to the second-order Doppler shift. For an rf trap this will be caused by the kinetic energy in the micromotion; for a Penning trap this will be caused by the kinetic energy in the magnetron motion (Wineland, 1983).

Optical frequency standards have the basic advantage of higher Q for fixed coherent interaction time. Dehmelt has proposed optical frequency standards based on forbidden transitions of single, laser-cooled group IIIA ions (Tl^+, In^+, Ga^+, Al^+, or B^+) stored in small rf traps (Dehmelt, 1982). Penning traps or Penning/rf trap combinations might also be used (Wineland and Itano, 1982b). The $6\,^2S_{1/2}-6\,^2P_{1/2}-5\,^2D_{3/2}$ Raman transition in Ba^+ could be used as a reference to generate a stable infrared difference frequency in a nonlinear crystal (Neuhauser *et al.*, 1981; Dehmelt, 1982). Also in Ba^+, the $5\,^2D_{5/2}$ to $5\,^2D_{3/2}$ 12-μm transition (Dehmelt *et al.*, 1982) and the quadrupole-allowed $6\,^2S_{1/2}$ to $5\,^2D_{5/2}$ 1.8-μm transition (Dehmelt, 1981b) have been proposed as standards. Other high-Q optical transitions in Sr^+ (Dehmelt and Walther, 1975), Pb^+, I^+, and Bi^+ (Strumia, 1978) have been suggested for stored ion frequency standards. The two-photon (Bender *et al.*, 1976; Wineland *et al.*, 1981a) or single-photon quadrupole (Wineland *et al.*, 1981b) $5d^{10}\,6s\,^2S_{1/2}$ to $5d^9\,6s^2\,^2D_{5/2}$ transition in Hg^+ has also been suggested. Two-photon transitions have the advantage of being first-order Doppler free even for a cloud of many ions, where it is impossible to satisfy

the Dicke criterion at optical wavelengths. They have the disadvantage that the large fields required to drive the transition cause ac Stark shifts.

E. Molecular Ion Spectroscopy

As the species under investigation becomes more complex, fewer of the trapped ions reside in the particular states of interest. Therefore, the fact that molecular spectroscopy is possible at all in the ion traps where so few ions are present is indeed remarkable. Nevertheless, the traps do provide some advantages over other methods for molecular ion spectroscopy. First, the environment in a high vacuum can provide cleaner operating conditions for the ions, thereby suppressing collision-induced chemical reactions. Because of the long storage times, the state distributions of ions can be allowed to relax, thus increasing the number of ions in a particular ground state. In addition, the traps (particularly the rf trap) can be operated in a mass-selective mode in order to reduce the effects of background ions. The use of LIF can also be used to "tag" certain ions for chemical studies.

The first successful molecular ion experiments measured high-resolution rf spectra of H_2^+ ions (Dehmelt and Jefferts, 1962; Jefferts, 1968, 1969; Richardson *et al.*, 1968; Menasian and Dehmelt, 1973). Transitions were detected by using the orientation dependence of photodissociation. These measurements were particularly interesting because they could be compared to high accuracy with theory. More recently, the group of Mahan has measured the spectra of heavier ions using LIF techniques (Grieman *et al.*, 1980, 1981a,b; see also Danon *et al.*, 1982). Dunbar and Beauchamp (Dunbar and Kramer, 1973; Freiser and Beauchamp, 1974; Dunbar *et al.*, 1977) have also used LIF for photodissociation studies.

VI. Negative Ion Spectroscopy

Negative ions have been observed to have only one, or at most a few, bound electronic states, in contrast to neutral or positively charged atoms or molecules, which have an infinite number. Therefore, line emission or absorption spectroscopy is not generally feasible. Most spectroscopy of negative ions is based on photodetachment (absorption of a photon with loss of an electron) or, for molecules, on photodissociation (absorption of a photon with fragmentation of the molecule). For more general reviews, including results of other experimental methods, such as ion beams and drift tubes, see the article by Hotop and Lineberger (1975) on atomic negative

ions, the articles by Corderman and Lineberger (1979) and by Janousek and Brauman (1979) on molecular negative ions, and the book by Massey (1976).

A. Atoms

The only spectroscopic studies of negative atomic ions to use ion storage techniques are those of Larson and co-workers. Perhaps this is because photodetachment cross sections and electron affinities can be determined using ion beams, either by using a tunable light source and observing the threshold wavelengths or by using a fixed-wavelength source and measuring the energies of the detached electrons. However, the long observation times available with trapped ions can be useful in high-resolution studies. Also,

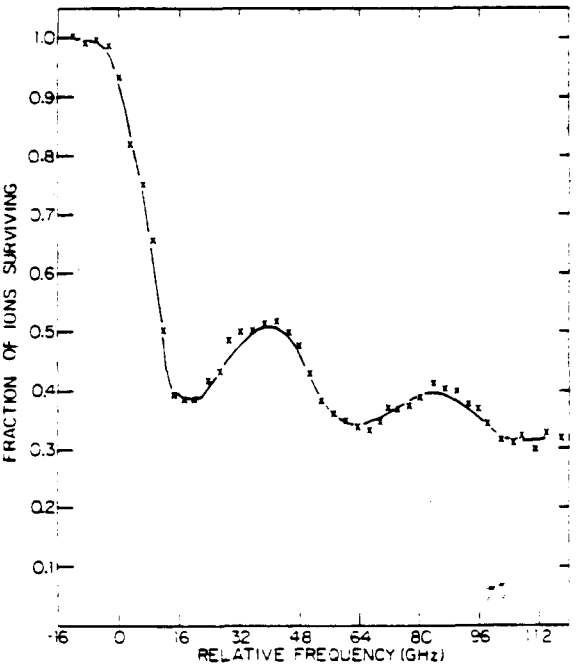

FIG. 21. Photodetachment data near the $S^-(^2P_{3/2}) \rightarrow S(^3P_2)$ threshold. The fraction of ions surviving laser illumination is plotted as a function of the light frequency (with an arbitrary zero). The light had π polarization and the magnetic field was 1.57 T. The solid curve is a theoretical prediction, with three parameters adjusted to give agreement with the data. (From Blumberg *et al.*, 1979.)

effects due to high magnetic fields can be conveniently studied in a Penning trap.

Near-threshold photodetachment of S^- was observed in a Penning trap in a magnetic field of the order of 1 T by Blumberg *et al.* (1978). The relative number of ions surviving after irradiation by a tunable cw dye laser was measured by resonantly exciting their axial motion and detecting the image current at the ring electrode at the second harmonic. The cross section was found to have an oscillatory dependence on light frequency, with a spacing between peaks approximately equal to the electron cyclotron frequency. These peaks correspond to thresholds for excitation of the detached electron to quantized cyclotron levels. The light polarization and frequency dependences of the cross sections are well described by a theory which ignores the final-state interaction between the detached electron and the neutral atom, but which includes the Zeeman splittings of the initial ionic state and the final atomic state and the broadening due to the Doppler effect and the motional electric field (Blumberg *et al.*, 1979) (see Fig. 21). The effect of including the final-state interaction in lowest order is to reduce the cross section near the thresholds (Larson and Stoneman, 1982).

Different magnetic sublevels have different cross sections for photode-

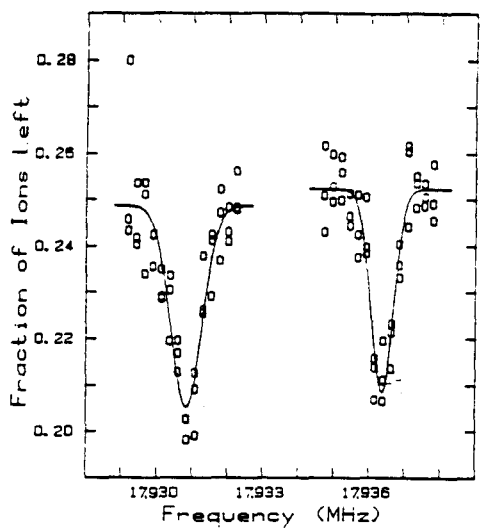

FIG. 22. Microwave Zeeman resonances between magnetic sublevels of the $^2P_{3/2}$ level of S^- at a magnetic field of about 0.96 T, observed by state-dependent photodetachment. The lower frequency transition is $m_J = -\frac{1}{2}$ to $m_J = -\frac{3}{2}$ and the higher frequency one is $m_J = +\frac{1}{2}$ to $m_J = +\frac{3}{2}$. (From Jopson and Larson, 1981.)

tachment by polarized light, a fact which can be used to detect microwave Zeeman transitions (Jopson and Larson, 1980). The magnetic moments of S^- (Jopson and Larson, 1981) and O^- (Larson and Jopson, 1981), and the hyperfine constants of $^{33}S^-$ (Jopson *et al.*, 1981) have been measured by this technique (see Fig. 22). In these experiments, the magnetic field is calibrated by driving the cyclotron resonance of electrons trapped alternately in the same apparatus.

B. Molecules

Larson and Stoneman (1982) have observed photodetachment of SeH^- near threshold, with a resolution of about 0.2 cm^{-1}. The rotational structure is well resolved. The oscillatory structure at the electron cyclotron frequency continues for many cycles, in contrast to the atomic case (see Fig. 23). This

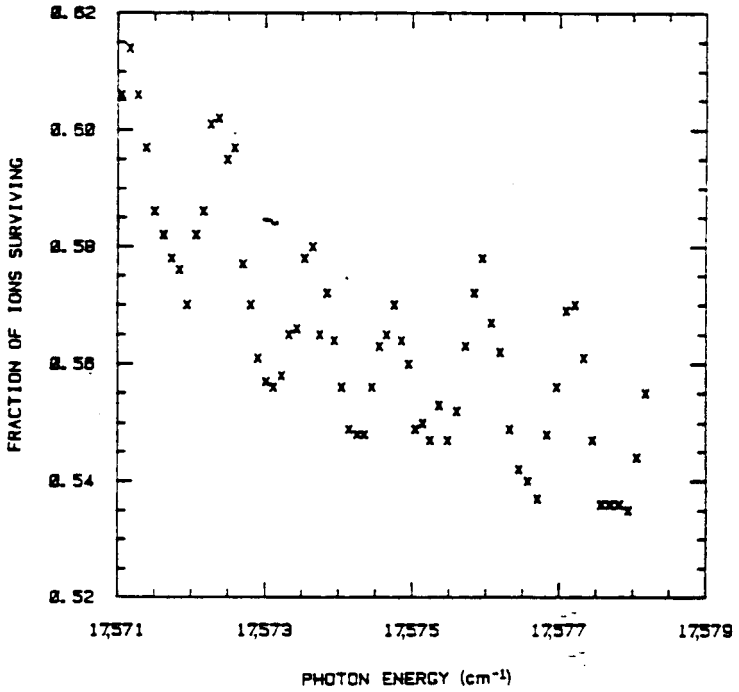

FIG. 23. Photodetachment data for SeH^- in the vicinity of a rotational ($J \rightarrow J'$) threshold. The magnetic field was 1.3 T. The oscillatory structure has a period at or very close to the electron cyclotron frequency.

may be due to the final-state interaction between the electron and the molecular electric dipole moment.

Photodetachment or photodissociation of many different negative molecular ions has been observed in ICR spectrometers (Smyth *et al.*, 1971; Eyler, 1974; Dunbar and Hutchinson, 1974). Most of this work has been done by Brauman and co-workers. The basic advantages of ICR techniques over beam techniques are the large variety of ions that can be produced by dissociative attachment, followed by ion–molecule reactions, and the long trapping times, which allow many of the excited states to decay before interrogation, thus simplifying the spectra. The quantities obtained are the electron affinities and some spectroscopic constants (vibrational, spin–orbit, etc.). Much of this work has been reviewed by Corderman and Lineberger (1979) and by Janousek and Brauman (1979). More recently, ICR techniques have been used to observe infrared multiphoton photodetachment (Rosenfeld *et al.*, 1979) and narrow resonances near threshold which may be due to Rydberg-like states bound by the electric dipole moment of the neutral molecule (Jackson *et al.*, 1979, 1981).

VII. Radiative Lifetime Measurements

For longer-lived states, the ion traps may be particularly well suited to make measurements of radiative lifetimes. Clearly this is a result of the relatively perturbation-free environment and the long storage times possible. This is indicated by the measurements of the lifetimes of the $5\ ^2D_{3/2}$ state in Ba^+, $\tau \cong 17.5$ sec (Schneider and Werth, 1979), the $5\ ^2D_{5/2}$ state in Ba^+, $\tau \cong 47$ sec (Plumelle *et al.*, 1980), and the $2\ ^3S_1$, state in Li^+, $\tau \cong 58.6$ sec (Knight and Prior, 1980: see also Osipowicz and Werth, 1981). Of particular interest for atomic physics are the lifetime measurements of Prior and colleagues at Berkeley on simple atomic ions since these can be compared with various theories. Lifetimes of $2\ ^1S_0$ Li^+($\tau \cong 503\ \mu$sec) in a Penning trap (Prior and Shugart, 1971), 2s He^+ ($\tau \cong 1.92$ msec) in a Kingdon trap (Prior, 1972), and $2\ ^3S_1$ Li^+ ($\tau \cong 58.6$ sec) in an rf trap (Knight and Prior, 1980) have been measured. More recently, lifetimes of atomic and molecular ions of atmospheric and astrophysical interest have been determined. For example, the lifetimes of the $^5S_2$ state of N^+ (Knight 1982) and the $^3P_1$ metastable level of Si^{2+} (Kwong *et al.*, 1983), and lifetimes in N_2^+ (Mahan and O'Keefe, 1981a,b) and CO^+ and CH^+ (Mahan and O'Keefe; 1981a,b; Danon *et al.*, 1982) have been measured.

ACKNOWLEDGMENTS

The authors wish to acknowledge many of the researchers in this field who have contributed information in the form of preprints, reprints, and private communications. We especially thank R. D. Knight, G. H. Dunn, J. J. Bollinger, and H. G. Dehmelt for their suggestions and comments on portions of the manuscript. Two of the authors (D.J.W.) and (W.M.I.) acknowledge the support of the Air Force Office of Scientific Research and the Office of Naval Research; the third author (R.S.V.) acknowledges the support of the National Science Foundation.

REFERENCES

André, J., and Vedel, F. (1977). *J. Phys. (Orsay, Fr.)* **38**, 1381.
André, J., Vedel, F., and Vedel, M. (1979). *J. Phys. (Orsay, Fr.)* **40**, L-633.
André, J., Teboul, A., Vedel, F., and Vedel, M. (1981). *J. Phys. (Orsay, Fr.)* **42**, C8-315.
Becker, W., Blatt, R., and Werth, G. (1981). *J. Phys. (Orsay, Fr.)* **42**, C8-339.
Bender, P. L., Hall, J. L., Garstang, R. H., Pichanick, F. M. J., Smith, W. W., Barger, R. L., and West, J. B. (1976). *Bull. Am. Phys. Soc.* [2] **21**, 599.
Benilan, M. N., and Audoin, C. (1973). *Int. J. Mass Spectrom. Ion Phys.* **11**, 421.
Blatt, R., and Werth, G. (1982). *Phys. Rev. A*[3] **25**, 1476.
Blatt, R., and Werth, G. (1983). *In* "Precision Measurements and Fundamental Constants, II" (B. N. Taylor and W. D. Phillip, eds.). *NBS Spec. Publ. (U.S.)* **617** (in press).
Blatt, R., Schmeling, U., and Werth, G. (1979). *Appl. Phys.* **20**, 295.
Blatt, R., Schnatz, H., and Werth, G. (1982). *Phys. Rev. Lett.* **48**, 1601.
Blumberg, W. A. M., Jopson, R. M., and Larson, D. J. (1978). *Phys. Rev. Lett.* **40**, 1320.
Blumberg, W. A. M., Itano, W. M., and Larson, D. J. (1979). *Phys. Rev. A* [3] **19**, 139.
Bollinger, J. J., and Wineland, D. J. (1983). To be published.
Bonner, R. F., March, R. E., and Durup, J. (1976). *Int. J. Mass Spectrom. Ion Phys.* **22**, 17.
Bonner, R. F., Fulford, J. E., March, R. E., and Hamilton, G. F. (1977). *Int. J. Mass Spectrom. Ion Phys.* **24**, 255.
Borodkin, A. S. (1978). *Zh. Tekh. Fiz.* **48**, 889: *Sov. Phys.—Tech. Phys. (Engl. Transl.)* **23**, 520.
Brown, L. S., and Gabrielse, G. (1982). *Phys. Rev. A* [3] **25**, 2423.
Bryne, J., and Farago, P. S. (1965). *Proc. Phys. Soc. London* **86**, 801.
Church, D. A. (1969). *J. Appl. Phys.* **40**, 3127.
Church, D. A. (1982). *In* "Physics of Electronic and Atomic Collisions" (S. Datz, ed.), p. 533. North-Holland Publ., Amsterdam.
Church, D. A., and Dehmelt, H. G. (1969). *J. Appl. Phys.* **40**, 3421.
Church, D. A., and Mokri, B. (1971). *Z. Phys.* **244**, 6.
Comisarow, M. B. (1981). *Int. J. Mass Spectrom. Ion Phys.* **37**, 251.
Corderman, R. R., and Lineberger, W. C. (1979). *Annu. Rev. Phys. Chem.* **30**, 347.
Coutandin, J., and Werth, G. (1982). *Appl. Phys. B* **29**, 89.
Cutler, L. S., Giffard, R. P., and McGuire, M. D. (1982). *NASA Conf. Publ.* **2220**, 563.
Danon, J., Mauclaire, G., Govers, T. R., and Marx, R. (1982). *J. Chem. Phys.* **76**, 1255.
Dawson, P. H. (1980). *Adv. Electron. Electron Phys.* Suppl. **13B**, 173.
Dawson, P. H., and Lambert, C. (1975). *Int. J. Mass. Spectrom. Ion Phys.* **16**, 269.
Dawson, P. H., and Whetten, N. R. (1968). *J. Vac. Sci. Technol.* **5**, 1.

deGrassie, J. S., and Malmberg, J. M. (1980). *Phys. Fluids* **23**, 63.
Dehmelt, H. G. (1956). *Phys. Rev.* **103**, 1125.
Dehmelt, H. G. (1958). *Phys. Rev.* **109**, 381.
Dehmelt, H. G. (1967). *Adv. At. Mol. Phys.* **3**, 53.
Dehmelt, H. G. (1969). *Adv. At. Mol. Phys.* **5**, 109.
Dehmelt, H. G. (1975). *In* "The Physics of Electronic and Atomic Collisions" (J. S. Risley and R. Geballe, eds.), p. 857. Univ. of Washington Press, Seattle.
Dehmelt, H. G. (1976). *In* "Atomic Masses and Fundamental Constants" (J. H. Sanders and A. H. Wapstra, eds.), 5th, p. 499. Plenum, New York.
Dehmelt, H. G. (1981a). *At. Phys.* **7**, 337.
Dehmelt, H. G. (1981b). *J. Phys. (Orsay, Fr.)* **42**, C8-299.
Dehmelt, H. (1982). *IEEE Trans. Instrum. Meas.* **IM-31**, 83.
Dehmelt, H. G. (1983). *In* "Advances in Laser Spectroscopy" (F.T. Arecchi, F. Strumia, and H. Walther, eds.). Plenum, New York.
Dehmelt, H. G., and Jefferts, K. B. (1962). *Phys. Rev.* **125**, 1318.
Dehmelt, H. G., and Major, F. G. (1962). *Phys. Rev. Lett.* **8**, 213.
Dehmelt, H. G., and Walls, F. L. (1968). *Phys. Rev. Lett.* **21**, 127.
Dehmelt, H. G., and Walther, H. (1975). *Bull. Am. Phys. Soc.* [2] **20**, 61.
Dehmelt, H. G., Schwinberg, P. B., and Van Dyck, R. S., Jr., (1978). *Int. J. Mass Spectrom. Ion Phys.* **26**, 107.
Dehmelt, H. G., Van Dyck, R. S., Jr., Schwinberg, P., and Gabrielse, G. (1979). *Bull. Am. Phys. Soc.* [2] **24**, 757.
Dehmelt, H., Nagourney, W., and Janik, G. (1982). *Bull. Am. Phys. Soc.* [2] **27**, 402.
Dicke, R. H. (1953). *Phys. Rev.* **89**, 472.
Donets, E. D., and Pikin, A. I. (1976). *Zh. Eksp. Teor. Fiz.* **70**, 2025; *Sov. Phys.—JETP (Engl. Transl.)* **43**, 1057.
Drullinger, R. E., Wineland, D. J., and Bergquist, J. C. (1980). *Appl. Phys.* **22**, 365.
Duchêne, J. L., Audoin, C., and Schermann, J. P. (1977). *Metrologia* **13**, 157.
Dunbar, R. C., and Hutchinson, B. B. (1974). *J. Am. Chem. Soc.* **96**, 1154.
Dunbar, R. C., and Kramer, J. M. (1973). *J. Chem. Phys.* **58**, 1266.
Dunbar, R. C., Fu, E. W., and Olah, G. A. (1977). *J. Am. Chem. Soc.* **99**, 7502.
Ekstrom, P., and Wineland, D. (1980). *Sci. Am.* **243**, No. 2, 104.
Eyler, J. R. (1974). *Rev. Sci. Instrum.* **45**, 1154.
Field, J. H., Picasso, E., and Combley, F. (1979). *Usp. Fiz. Nauk* **127**, 553; *Sov. Phys.—Usp. (Engl. Transl.)* **22**, 199.
Fisher, E. (1959). *Z. Phys.* **156**, 1.
Fortson, E. N., Major, F. G., and Dehmelt, H. (1966). *Phys. Rev. Lett.* **16**, 221.
Freiser, B. J., and Beauchamp, J. L. (1974). *J. Am. Chem. Soc.* **96**, 6260.
Gaboriaud, M. N., Desaintfuscien, M., and Major, F. G. (1981). *Int. J. Mass Spectrom. Ion Phys.* **41**, 109.
Gabrielse, G., and Dehmelt, H. G. (1980). *Bull. Am. Phys. Soc.* [2] **25**, 1149.
Gabrielse, G., and Dehmelt, H. G. (1983). *In* "Precision Measurements and Fundamental Constants. II" (B. N. Taylor and W. D. Phillips, eds.). *NBS Spec. Publ. (U.S.)* **617** (in press).
Gärtner G., and Klempt, E. (1978) *Z. Phys. A* **287**, 1.
Gilleland J. R., and Rich, A. (1972). *Phys. Rev. A* [3] **5**, 38.
Gräff, G. (1982). *Z. Phys. A* **305**, 107.
Gräff, G., and Holzscheiter, M. (1980). *Phys. Lett. A* **79A**, 380.
Gräff, G., and Major, F. G., Roeder, R. W. H., and Werth, G. (1968). *Phys. Rev. Lett.* **21**, 340.
Gräff, G., Klempt, E., and Werth, G. (1969). *Z. Phys.* **222**, 201.
Gräff, G., Huber, K., Kalinowsky, H., and Wolf, H. (1972). *Phys. Lett. A* **41A**, 277.

Gräff, G., Kalinowsky, H., and Traut, J. (1980). *Z. Phys.* **297**, 35.
Gräff, G., Kalinowsky, H., and Traut, J. (1983). *In* "Precision Measurements and Fundamental Constants. II" (B. N. Taylor and W. D. Phillips, eds.). *NBS Spec. Publ. (U.S.)* **617** (in press).
Grieman, F. J., Mahan, B. H., and O'Keefe, A. (1980). *J. Chem. Phys.* **72**, 4246.
Grieman, F. J., Mahan, B. H., and O'Keefe, A. (1981a). *J. Chem. Phys.* **74**, 857.
Grieman, F. J., Mahan, B. H., O'Keefe, A., and Winn, J. S. (1981b). *Faraday Discuss. Chem. Soc.* **71**, 191.
Hamdan, M., Birkinshaw, K., and Hasted, J. B. (1978). *J. Phys. B* **11**, 331.
Hänsch, T. W., and Schawlow, A. L. (1975). *Opt. Commun.* **13**, 68.
Harrison, E. R. (1959). *Am. J. Phys.* **27**, 314.
Hasted, J. B., and Awad, G. L. (1972). *J. Phys. B* **5**, 1719.
Haught, A. F., and Polk, D. H. (1966). *Phys. Fluids* **9**, 2047.
Hooverman, R. M. (1963). *J. Appl. Phys.* **34**, 3505.
Hotop, H., and Lineberger, W. C. (1975). *J. Phys. Chem. Ref. Data* **4**, 539.
Iffländer, R., and Werth, G. (1977a). *Metrologia* **13**, 167.
Iffländer, R., and Werth, G. (1977b). *Opt. Commun.* **21**, 411.
Itano, W. M., and Wineland, D. J. (1981). *Phys. Rev. A* [3] **24**, 1364.
Itano, W. M., and Wineland, D. J. (1982). *Phys. Rev. A* [3] **25**, 35.
Jackson, R. L., Zimmerman, A. H., and Brauman, J. I. (1979). *J. Chem. Phys.* **71**, 2088.
Jackson, R. L., Hiberty, P. C., and Brauman, J. I. (1981). *J. Chem. Phys.* **74**, 3705.
Janousek, B. K., and Brauman, J. I. (1979). *In* "Gas Phase Ion Chemistry" (M. T. Bowers, Vol. 2, ed.), pp. 53–86. Academic Press New York.
Jardino, M., and Desaintfuscien, M. (1980). *IEEE Trans. Instrum. Meas.* **IM-29**, 163.
Jardino, M., Desaintfuscien, M., Barillet, R., Viennet, J. Petit, P., and Audoin, C. (1981a). *Appl. Phys.* **24**, 107.
Jardino, M., Desaintfuscien, M., and Plumelle, F. (1981b). *J. Phys. (Orsay, Fr.)* **42**, C8-327.
Javanainen, J. (1980). *Appl. Phys.* **23**, 175.
Javanainen, J. (1981a). *J. Phys. B* **14**, 2519.
Javanainen, J. (1981b). *J. Phys. B* **14**, 4191.
Javanainen, J. and Stenholm, S. (1980). *Appl. Phys.* **21**, 283.
Javanainen, J. and Stenholm, S. (1981a). *Appl. Phys.* **24**, 71.
Javanainen, J. and Stenholm, S. (1981b). *Appl. Phys.* **24**, 151.
Jefferts, K. B. (1968). *Phys. Rev. Lett.* **20**, 39.
Jefferts, K. B. (1969). *Phys. Rev. Lett.* **23**, 1476.
Jeffries, J. B. (1980). Ph. D. thesis, University of Colorado, Boulder.
Johnson, C. E. (1983). *Bull. Am. Phys. Soc.* [2] **28**, 796.
Jopson, R. M., and Larson, D. J. (1980). *Opt. Lett.* **5**, 531.
Jopson, R. M., and Larson, D. J. (1981). *Phys. Rev. Lett.* **47**, 789.
Jopson, R. M., and Trainham, R., and Larson, D. J. (1981). *Bull. Am. Phys. Soc.* [2] **26**, 1306.
Kienow, E., Klempt, E., Lange, F., and Neubecker, K. (1974). *Phys. Lett. A* **46A**, 441.
Kingdon, K. H. (1923). *Phys. Rev.* **21**, 408.
Kinoshita, T., and Lindquist, W. B. (1981). *Phys. Rev. Lett.* **47**, 1573.
Knight, R. D. (1981). *Appl. Phys. Lett.* **38**, 221.
Knight, R. D. (1982). *Phys. Rev. Lett.* **48**, 792.
Knight, R. D. (1983). *Int. J. Mass Spectrom. Ion Phys.* (*In press*).
Knight, R. D., and Prior, M. H. (1979). *J. Appl. Phys.* **50**, 3044.
Knight, R. D., and Prior, M. H. (1980). *Phys. Rev. A* [3] **21**, 179.
Kwong, H. S., Johnson, B. C., Smith, P. L., and Parkinson, W. H. (1983). *Phys. Rev. A* [3] **27**, 3040.
Lakkaraju, H. S., and Schuessler, H. A. (1982). *J. Appl. Phys.* **53**, 3967.

Larson, D. J., and Jopson, R. M. (1981). *Springer Ser. Opt. Sci.* **30**, 369.
Larson, D. J., and Stoneman, R. (1982). *J. Phys. (Orsay. Fr.)* **43**, C2-285.
Lewis, R. R. (1982). *J. Appl. Phys.* **53**, 3975.
Lewis, R. R. (1983) *Phys. Rev. A (in press).*
Liebes, S., Jr., and Franken, P. (1959). *Phys. Rev.* **116**, 633.
McGuire, M. D., and Fortson, E. N. (1974). *Phys. Rev. Lett.* **33**, 737.
McGuire, M. D., Petsch, R., and Werth, G. (1978). *Phys. Rev. A* [3] **17**, 1999.
McIlraith, A. H. (1971). *J. Vac. Sci. Technol.* **9**, 209.
McIver, R. T., Jr. (1970). *Rev. Sci. Instrum.* **41**, 555.
McIver, R. T., Jr. (1978a). *Lect. Notes Chem.* **7**, 97.
McIver, R. T., Jr. (1978b). *Rev. Sci. Instrum.* **49**, 111.
McLachlan, N. W. (1947). "Theory and Application of Mathieu Functions." Oxford Univ. Press (Clarendon), London and New York.
Mahan, B. H., and O'Keefe, A. (1981a). *J. Chem. Phys.* **74**, 5606.
Mahan, B. H., and O'Keefe, A (1981b). *Astrophys. J.* **248**, 1209.
Major, F. G. (1977). *J. Phys. (Orsay, Fr.)* **38**, L-221.
Major, F. G., and Dehmelt, H. G. (1968). *Phys. Rev.* [2] **170**, 91.
Major, F. G., and Duchêne, J. L. (1975). *J. Phys. (Orsay, Fr.)* **36**, 953.
Major, F. G., and Schermann, J. P. (1971). *Bull. Am. Phys. Soc.* [2] **16**, 838.
Major, F. G., and Werth, G. (1973). *Phys. Rev. Lett.* **30**, 1155.
Major, F. G., and Werth, G. (1978). *Appl. Phys.* **15**, 201.
Maleki, L. (1981). *NASA Conf. Publ.* **2220**, 593.
Malmberg, J. H., and Driscoll, C. F. (1980). *Phys. Rev. Lett.* **44**, 654.
Massey, H. S. W. (1976). "Negative Ions," 3rd ed. Cambridge Univ. Press, London and New York.
Mather, R. E., Waldren, R. M., Todd, J. F. J., and March, R. E. (1980). *Int. J. Mass Spectrom. Ion Phys.* **33**, 201.
Menasian, S. C., and Dehmelt, H. G. (1973). *Bull. Am. Phys. Soc.* [2] **18**, 408.
Minogin, V. G. (1982). *Usp. Fiz. Nauk* 137, 173 [*Sov. Phys. Usp.* **25**, 359—*Engl. Transl.*]
Nagourney, W., and Dehmelt, H. G. (1981a). *Bull. Am. Phys. Soc.* [2] **26**, 797.
Nagourney, W., and Dehmelt, H. (1981b). *Bull. Am. Phys. Soc.* [2] **26**, 805.
Nagourney, W., Janik, G., and Dehmelt, H. (1982). *Bull. Am. Phys. Soc.* [2] **27**, 839.
Nagourney, W., Janik, G., and Dehmelt, H. (1983). *Proc. Natl. Acad. Sci.* U.S.A. **80**, 643.
Neuhauser, W., Hohenstatt, M., Toschek, P., and Dehmelt, H. G. (1978a). *Phys. Rev. Lett.* **41**, 233.
Neuhauser, W., Hohenstatt, M., Toschek, P., and Dehmelt, H. (1978b). *Appl. Phys.* **17**, 123.
Neuhauser, W., Hohenstatt, M., Toschek, P., and Dehmelt, H. (1980). *Phys. Rev. A* [3] **22**, 1137.
Neuhauser, W., Hohenstatt, M., Toschek, P., and Dehmelt, H. (1981). *In* "Spectral Line Shapes" (B. Wende, ed.), Vol. 5, p. 1045. De Gruyter, Hawthorne, New York.
O, C. S., and Schuessler, H. A. (1980a). *Int. J. Mass Spectrom. Ion Phys.* **35**, 305.
O, C. S., and Schuessler, H. A. (1980b). *J. Appl. Phys.* **52**, 2601.
O, C. S., and Schuessler, H. A. (1981). *Int. J. Mass Spectrom. Ion Phys.* **39**, 95.
O, C. S., and Schuessler, H. A. (1982). *Rev. Phys. Appl.* **17**, 83.
O, C. S., and Gärtner, G. F., and Schuessler, H. A. (1982). *Appl. Phys. Lett.* **41**, 33.
O'Neil, T. M., and Driscoll, C. F. (1979). *Phys. Fluids* **22**, 266.
Osipowicz, A., and Werth, G. (1981). *Opt. Commun.* **36**, 359.
Owe Berg, T. G., and Gaukler, T. (1969) *Am. J. Phys.* **37**, 1013.
Penning, F. M. (1936). *Physica* **3**, 873.
Phillips, W. D., Cooke, W. E., and Kleppner, D. (1977). *Metrologia* **13**, 179.

Plumelle, F. (1979). Ph. D. thesis. Université de Paris-Sud, Orsay.
Plumelle, F., Desaintfuscien, M., Duchêne, J. J., and Audoin, C. (1980). *Opt. Commun.* **34**, 71.
Prasad, S. A., and O'Neil, T. M. (1979). *Phys. Fluids* **22**, 278.
Prior, M. H. (1972). *Phys. Rev. Lett.* **29**, 611.
Prior, M. H., and Knight, R. D. (1980). *Opt. Commun.* **35**, 54.
Prior, M. H., and Shugart, H. A. (1971). *Phys. Rev. Lett.* **27**, 902.
Prior, M. H., and Wang, E. C. (1977). *Phys. Rev. A* [3] **16**, 6.
Ramsey, N. F. (1956). "Molecular Beams." Oxford Univ. Press, London and New York.
Redhead, P. A. (1967). *Can. J. Phys.* **45**, 1791.
Rich, A. (1968a). *Phys. Rev. Lett.* **20**, 967.
Rich, A. (1968b). *Phys. Rev. Lett.* **21**, 1221.
Rich, A., and Wesley, J. C. (1972). *Rev. Mod. Phys.* **44**, 250.
Richardson, C. B., Jefferts, K. B., and Dehmelt, H. G. (1968). *Phys. Rev.* [2] **165**, 80.
Rosenfeld, R. N., Jasinski, J. M., and Brauman, J. I. (1979). *J. Chem. Phys.* **71**, 1030.
Ruster, W., Bonn, J., Peuser, P., and Trautmann, N. (1983). *Appl. Phys.* **B30**, 83.
Schaaf, H., Schmeling, U., and Werth, G. (1981). *Appl. Phys.* **25**, 249.
Schneider, R., and Werth, G. (1979). *Z. Phys. A* **293**, 103.
Schuessler, H. A. (1971a). *Metrologia* **7**, 103.
Schuessler, H. A. (1971b). *Appl. Phys. Lett.* **18**, 117.
Schuessler, H. A. (1979). *In* "Physics of Atoms and Molecules, Progress in Atomic Spectroscopy" (W. Hanle and H. Kleinpoppen, eds.), p. 999. Plenum, New York.
Schuessler, H. A. (1980). *In* "Physics of Atoms and Molecules, Coherence and Correlation in Atomic Collisions" (H. Kleinpoppen and J. F. Williams, eds.), p. 423. Plenum, New York.
Schuessler, H. A., and O, C. S. (1981). *Nucl. Instrum. Methods* **186**, 219.
Schuessler, H. A., Fortson, E. N., and Dehmelt, H. G. (1969). *Phys. Rev* [2] **187**, 5.
Schwinberg, P. B., Van Dyck, R. S., Jr., and Dehmelt, H. G. (1981a). *Phys. Rev. Lett.* **47**, 1679.
Schwinberg, P. B., Van Dyck, R. S., Jr., and Dehmelt, H. G. (1981b). *Bull. Am. Phys. Soc.* [2] **26**, 597.
Schwinberg, P. B., Van Dyck, R. S., Jr., and Dehmelt, H. G. (1981c). *Phys. Lett. A* **81A**, 119.
Schwinberg, P. B., Van Dyck, R. S., Jr., and Dehmelt, H. G. (1983). *In* "Precision Measurements and Fundamental Constants. II" (B. N. Taylor and W. D. Phillips, eds.). *NBS Spec. Publ. (U.S.)* **617** (in press).
Smith, L. G., and Wapstra, A. H. (1975). *Phys. Rev. C* [3] **11**, 1392.
Smyth, K. C., McIver, R. T., Jr., Brauman, J. I., and Wallace, R. W. (1971). *J. Chem. Phys.* **54**, 2758.
Sokolov, A. A., and Pavlenko, Yu. G. (1967). *Opt. Spectrosc.* **22**, 1.
Strumia, F. (1978). *Proc. 32nd Ann. Symp. Freq. Control* p. 444.
Taylor, B. N. (1976). *Metrologia* **12**, 81.
Todd, J. F. J., Lawson, G., and Bonner, R. F. (1976). *In* "Quadrupole Mass Spectroscopy and its Applications" (P. H. Dawson, ed.), Chapter VIII. Elsevier, Amsterdam.
Todd, J. F. J., Waldren, R. M., and Mather, R. E. (1980a). *Int. J. Mass Spectrom. Ion Phys.* **34**, 325.
Todd, J. F. J., Waldren, R. M., Freer, D. A., and Turner, R. B. (1980b). *Int. J. Mass Spectrom. Ion Phys.* **75**, 107.
Torelli, G. (1980). *Proc. Eur. Symp. Nucleon. Anti Nucleon Interact., 5th, 1980* p. 43.
Toschek, P. E., and Neuhauser, W. (1981). *At. Phys.* **7**, 529.
Van Dyck, R. S., Jr., and Schwinberg, P. B. (1981a). *Phys. Rev. Lett.* **47**, 395.
Van Dyck, R. S., Jr., and Schwinberg, P. B. (1981b). *Bull. Am. Phys. Soc.* [2] **26**, 796.
Van Dyck, R. S., Jr., and Schwinberg, P. B. (1983). *In* "Precision Measurements and Funda-

mental Constants. II" (B. N. Taylor and W. D. Phillips, eds.). *NBS Spec. Publ. (U.S.)* **617** (in press).
Van Dyck, R. S., Jr., Wineland, D. J., Ekström, P. A., and Dehmelt, H. G. (1976). *Appl. Phys. Lett.* **28**, 446.
Van Dyck, R. S., Jr., Schwinberg, P. B., and Dehmelt, H. G. (1977). *Phys. Rev. Lett.* **38**, 310.
Van Dyck, R. S., Jr., Schwinberg, P. B., and Dehmelt, H. G. (1978). *In* "New Frontiers in High-Energy Physics" (B. M. Kursunoglu, A. Perlmutter, and L. F. Scott, eds.), p. 159. Plenum, New York.
Van Dyck, R. S., Jr., Schwinberg, P. B., and Dehmelt, H. G. (1979). *Bull. Am. Phys. Soc.* [2] **24**, 758.
Van Dyck, R. S., Jr., Schwinberg, P. B., and Bailey, S. H. (1980). *In* "Atomic Masses and Fundamental Constants" (J. A. Nolen, Jr. and W. Benenson, eds.), 6th, p. 173. Plenum, New York.
Vane, C. R., Prior, M. H., and Marrus, R. (1981). *Phys. Rev. Lett.* **46**, 107.
Vedel, F., André, J., and Vedel, M. (1981). *J. Phys. (Orsay, Fr.)* **42**, 1611.
Vedel, F., André, J., Vedel, M., and Brincourt, G. (1983). *Phys. Rev. A* [3] **27**, 2321.
Vedel, M. (1976). *J. Phys. (Orsay, Fr.)* **37**, L-339.
Vedel, M., André, J., Chaillat-Negrel, S., and Vedel, F. (1981). *J. Phys. (Orsay, Fr.)* **42**, 541.
Walls, F. L. (1970). Ph. D. thesis, University of Washington, Seattle.
Walls, F. L., and Dunn, G. H. (1974). *Phys. Today* **27**, No. 8, 30.
Walls, F. L., and Stein, T. S. (1973). *Phys. Rev. Lett.* **31**, 975.
Werth, G. (1982). *Acta Phys. Polonica* **A61**, 213.
Wesley, J. C., and Rich, A. (1971). *Phys. Rev. A* [3] **4**, 1341.
Wilkinson, D. T., and Crane, H. R. (1963). *Phys. Rev.* **130**, 852.
Williams, E. R., and Olsen, P. T. (1979). *Phys. Rev. Lett.* **42**, 1575.
Wineland, D. J. (1979). *J. Appl. Phys.* **50**, 2528.
Wineland, D. J. (1983). *In* "Precision Measurements and Fundamental Constants. II" (B. N. Taylor and W. D. Phillips, eds.). *NBS Spec. Publ. (U.S.)* **617** (in press).
Wineland, D. J., and Dehmelt, H. G. (1975a). *J. Appl. Phys.* **46**, 919.
Wineland, D. J., and Dehmelt, H. G. (1975b). *Bull. Am. Phys. Soc.* [2] **20**, 637.
Wineland, D. J., and Dehmelt, H. G. (1975c). *Int. J. Mass Spectrom. Ion Phys.* **16**, 338; erratum: **19**, 251 (1976).
Wineland, D. J., and Itano, W. M. (1979). *Phys. Rev. A* [3] **20**, 1521.
Wineland, D. J., and Itano, W. M. (1981). *Phys. Lett. A* **82A**, 75.
Wineland, D. J., and Itano, W. M. (1982a). *Bull. Am. Phys. Soc.* [2] **27**, 471.
Wineland, D. J., and Itano, W. M. (1982b). *Bull. Am. Phys. Soc.* [2] **27**, 864.
Wineland, D. J., Ekstrom, P., and Dehmelt, H. (1973). *Phys. Rev. Lett.* **31**, 1279.
Wineland, D. J., Drullinger, R. E., and Walls, F. L. (1978). *Phys. Rev. Lett.* **40**, 1639.
Wineland, D. J., Bergquist, J. C., Itano, W. M., and Drullinger, R. E. (1980). *Opt. Lett.* **5**, 245.
Wineland, D. J., Itano, W. M., Bergquist, J. C., and Walls, F. L. (1981a). *Proc. 35th Annu. Symp. Freq. Control* p. 602 (copies available from Electronic Industries Assoc., 2001 Eye St., NW, Washington, DC 20006).
Wineland, D. J., Bergquist, J. C., Drullinger, R. E., Hemmati, H., Itano, W. M., and Walls, F. L. (1981b). *J. Phys. (Orsay, Fr.)* **42**, C8-307.
Wineland, D. J., Bollinger, J. J., and Itano, W. M. (1983). *Phys. Rev. Lett.* **50**, 628; erratum: **50**, 1333 (1983).
Wuerker, R. F., Shelton, H., and Langmuir, R. V. (1959a). *J. Appl. Phys.* **30**, 342.
Wuerker, R. F., Goldenberg, H. M., and Langmuir, R. V. (1959b). *J. Appl. Phys.* **30**, 441.
Zaritskii, A. A., Zukharov, S. O., and Kryukov, P. G. (1971). *Sov. Phys.—Tech. Phys. (Engl. Transl.)* **16**, 174.